Analyses chimiques quantitatives EDS au MEB par la méthode des f ratios et par la méthode de corrélation

Pr. Raynald Gauvin, Ph.D.
Nicolas Brodusch, M.Sc.A

McGill

Montréal, Québec,
Canada.

CASINO

https://www.memrg.com/programs-download

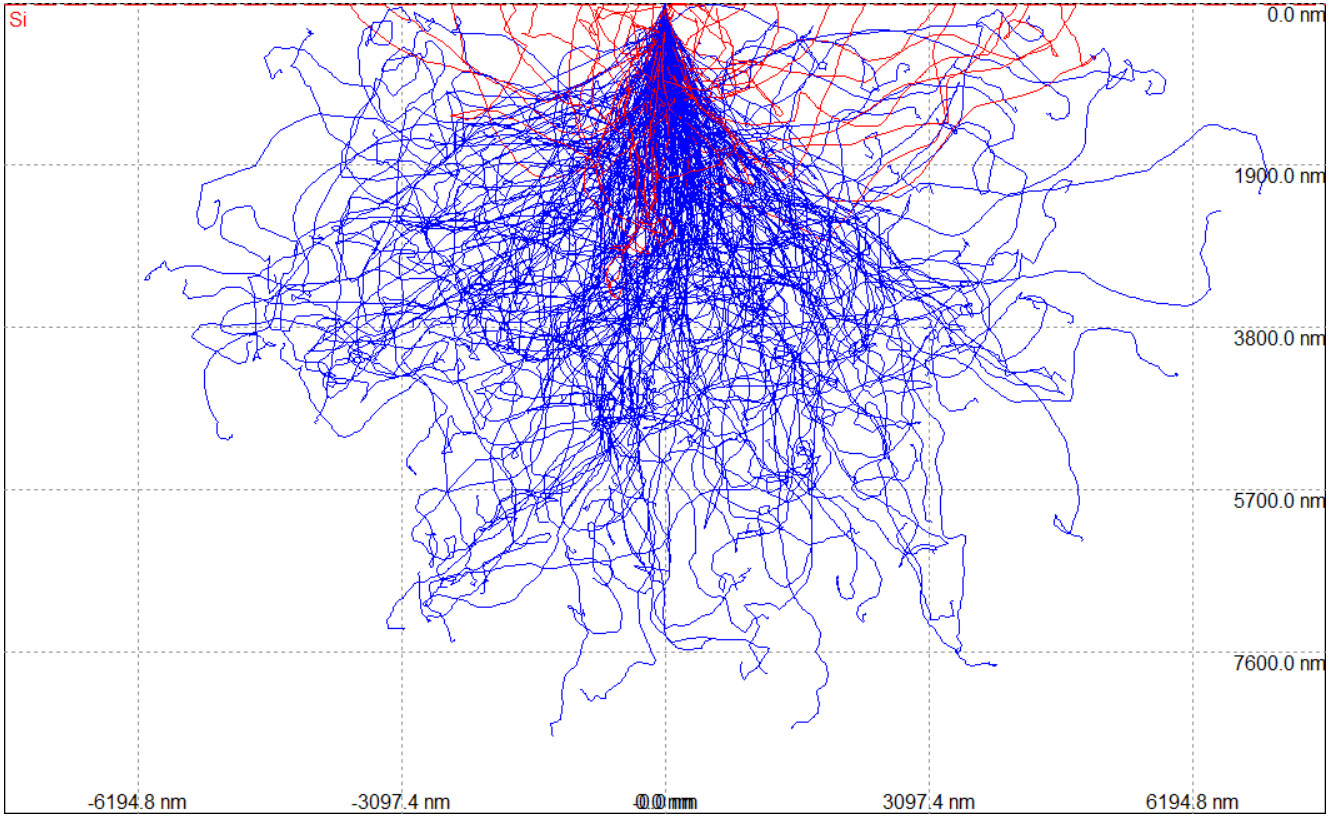

CASINO: A new Monte Carlo code in C language for electron beam interaction .1. Description of the program

P. Hovington, D. Drouin and R. Gauvin, SCANNING Volume: 19 Issue: 1 Pages: 1-14, 1997

913 Citations Google Scholar (3/11/25)

CASINO V2.42 - A fast and easy-to-use modeling tool for scanning electron microscopy and microanalysis users

D. Drouin, A. R. Couture, D. Joly, and R. Gauvin, SCANNING Volume: 29 Issue: 3 Pages: 92-101, 2007

1960 Citations Google Scholar (3/11/25)

WIN X-Ray

https://www.memrg.com/programs-download

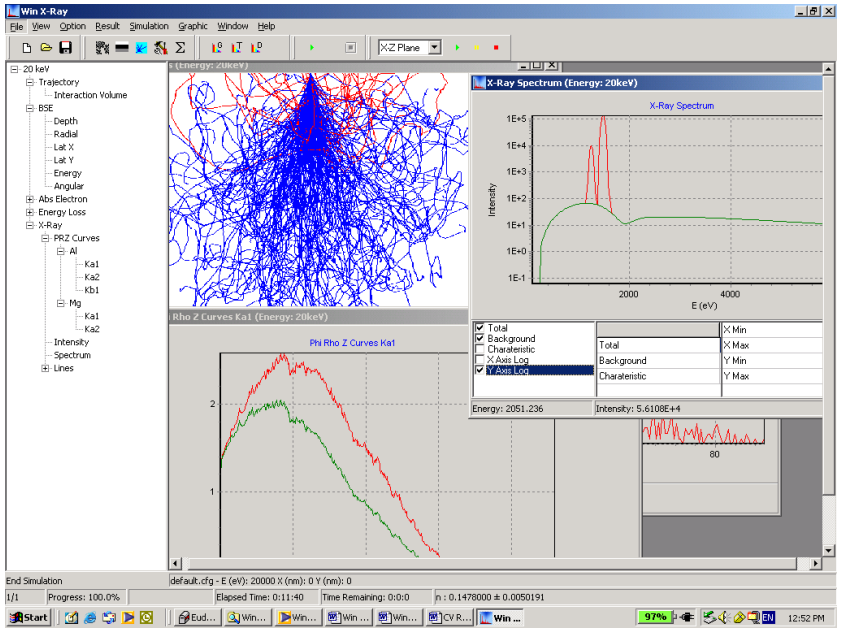

Microsc. Microanal. 12, 49–64, 2006
DOI: 10.1017/S1431927606060089

Microscopy AND Microanalysis

Win X-ray: A New Monte Carlo Program that Computes X-ray Spectra Obtained with a Scanning Electron Microscope

Raynald Gauvin,[1,*] Eric Lifshin,[2] Hendrix Demers,[1] Paula Horny,[1] and Helen Campbell[1]

[1]*Department of Metals and Materials Engineering, McGill University, Montréal, Québec H3A 2B2, Canada*
[2]*College of Nanoscale Science and Engineering, University at Albany, CESTM, 251 Fuller Road, Albany, NY 12203, USA*

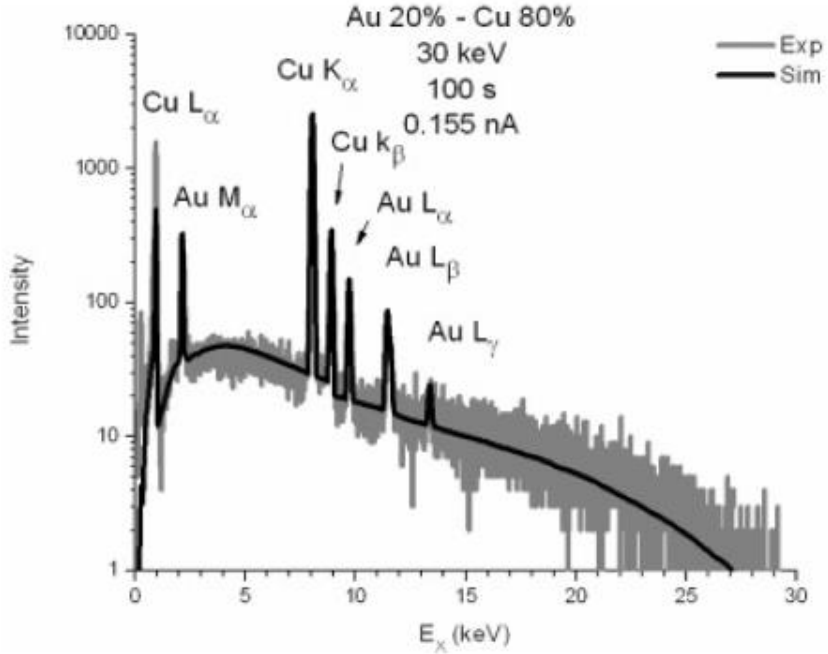

Figure 16. Comparison between a simulated (Sim) and a measured (Exp) Au (20 wt%)–Cu (80 wt%) X-ray spectrum obtained at 30 keV. See the text for details.

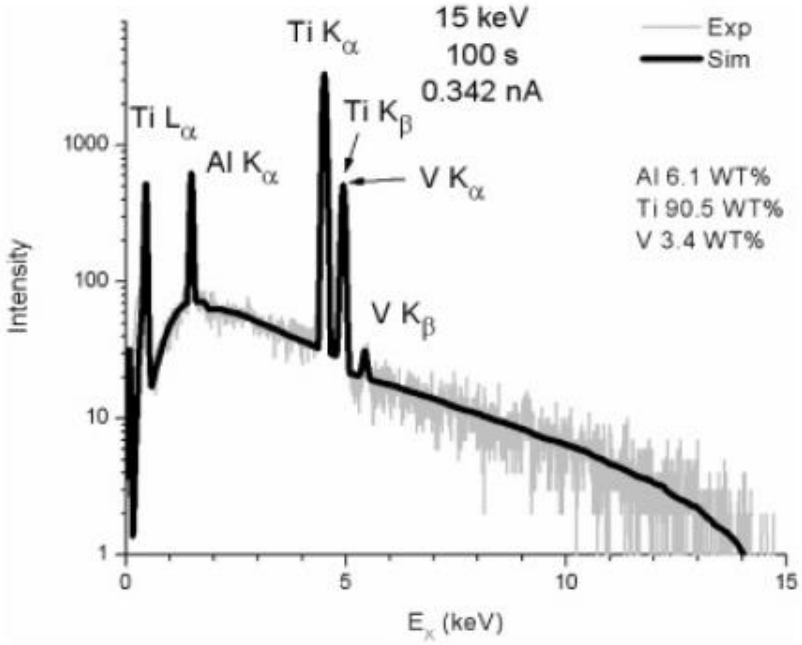

Figure 18. Comparison between a simulated (Sim) and a measured (Exp) Ti (90.5 wt%)–Al (6.1 wt%)–V (3.4 wt%) X-ray spectrum obtained at 15 keV. See the text for details.

Microanalyse Quantitative par Rayons-X - Étalons

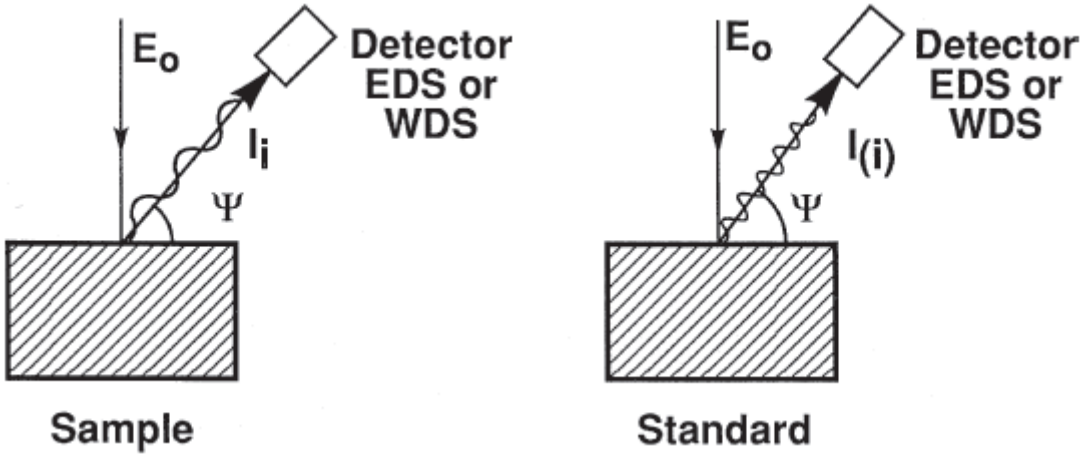

Les mesures d'intensité, tant pour l'échantillon que pour l'étalon, sont effectuées dans des conditions identiques : courant et durée d'acquisition identiques.

Les échantillons doivent présenter une composition homogène.

Les échantillons doivent avoir une surface plane.

Microanalyse quantitative par Rayons X

$$\frac{C_i}{C_{(i)}} = Z_i A_i F_i \frac{I_i}{I_{(i)}}$$

- Meilleure méthode chimique quantitative, précisions de 1 % obtenues sur la microsonde électronique.
- Les facteurs de correction ZAF sont obtenus à l'aide de modèles analytiques basés sur des simulations de Monte Carlo.

Pouchou Database (1988)
820 K ratios mesurés

1 - Analysed element (A)
2 - Line
3 - Companion (B)
4 - Accelerating voltage
5 - Weight fraction of A
6 - K-ratio of A
7 - X-ray take-off angle

$$K_i = \frac{I_i}{I_{(i)}}$$

	1	2	3	4	5	6	7
1	Al	Ka	Fe	20.0	.2410	.1240	52.5
2	Al	Ka	Fe	25.0	.2410	.0980	52.5
3	Al	Ka	Fe	30.0	.2410	.0830	52.5
4	Fe	Ka	Al	20.0	.7590	.7360	52.5
5	Fe	Ka	Al	25.0	.7590	.7420	52.5
6	Fe	Ka	Al	30.0	.7590	.7480	52.5
7	Fe	Ka	S	10.0	.4660	.4060	75.0
8	Fe	Ka	S	12.0	.4660	.4210	75.0
9	Fe	Ka	S	15.0	.4660	.4250	75.0
10	Fe	Ka	S	20.0	.4660	.4250	75.0
11	Fe	Ka	S	25.0	.4660	.4220	75.0
12	Fe	Ka	S	30.0	.4660	.4190	75.0
13	Al	Ka	B	4.0	.5551	.5150	40.0
14	Al	Ka	B	6.0	.5551	.5178	40.0
15	Al	Ka	B	8.0	.5551	.5188	40.0
16	Al	Ka	B	10.0	.5551	.5200	40.0
17	Al	Ka	B	12.0	.5551	.5198	40.0
18	Al	Ka	B	15.0	.5551	.5170	40.0
19	Al	Ka	B	20.0	.5551	.5130	40.0
20	Al	Ka	B	25.0	.5551	.5080	40.0
21	Al	Ka	B	30.0	.5551	.5030	40.0
22	Al	Ka	B	4.0	.1722	.1500	40.0
23	Al	Ka	B	6.0	.1722	.1502	40.0
24	Al	Ka	B	8.0	.1722	.1503	40.0
25	Al	Ka	B	10.0	.1722	.1503	40.0

	1	2	3	4	5	6	7
26	Al	Ka	B	12.0	.1722	.1503	40.0
27	Al	Ka	B	15.0	.1722	.1504	40.0
28	Al	Ka	B	20.0	.1722	.1495	40.0
29	Al	Ka	B	25.0	.1722	.1490	40.0
30	Al	Ka	B	30.0	.1722	.1455	40.0
31	Si	Ka	B	4.0	.4780	.4465	40.0
32	Si	Ka	B	6.0	.4780	.4528	40.0
33	Si	Ka	B	8.0	.4780	.4580	40.0
34	Si	Ka	B	10.0	.4780	.4622	40.0
35	Si	Ka	B	12.0	.4780	.4658	40.0
36	Si	Ka	B	15.0	.4780	.4696	40.0
37	Si	Ka	B	20.0	.4780	.4738	40.0
38	Si	Ka	B	25.0	.4780	.4758	40.0
39	Si	Ka	B	30.0	.4780	.4760	40.0
40	Si	Ka	B	4.0	.3143	.2900	40.0
41	Si	Ka	B	6.0	.3143	.2940	40.0
42	Si	Ka	B	8.0	.3143	.2978	40.0
43	Si	Ka	B	10.0	.3143	.3002	40.0
44	Si	Ka	B	12.0	.3143	.3036	40.0
45	Si	Ka	B	15.0	.3143	.3072	40.0
46	Si	Ka	B	20.0	.3143	.3120	40.0
47	Si	Ka	B	25.0	.3143	.3140	40.0
48	Si	Ka	B	30.0	.3143	.3156	40.0
49	Ti	Ka	B	6.0	.8322	.7922	40.0
50	Ti	Ka	B	8.0	.8322	.7937	40.0

Quantitative X-Ray Microanalysis
Pouchou Data Base (1988)

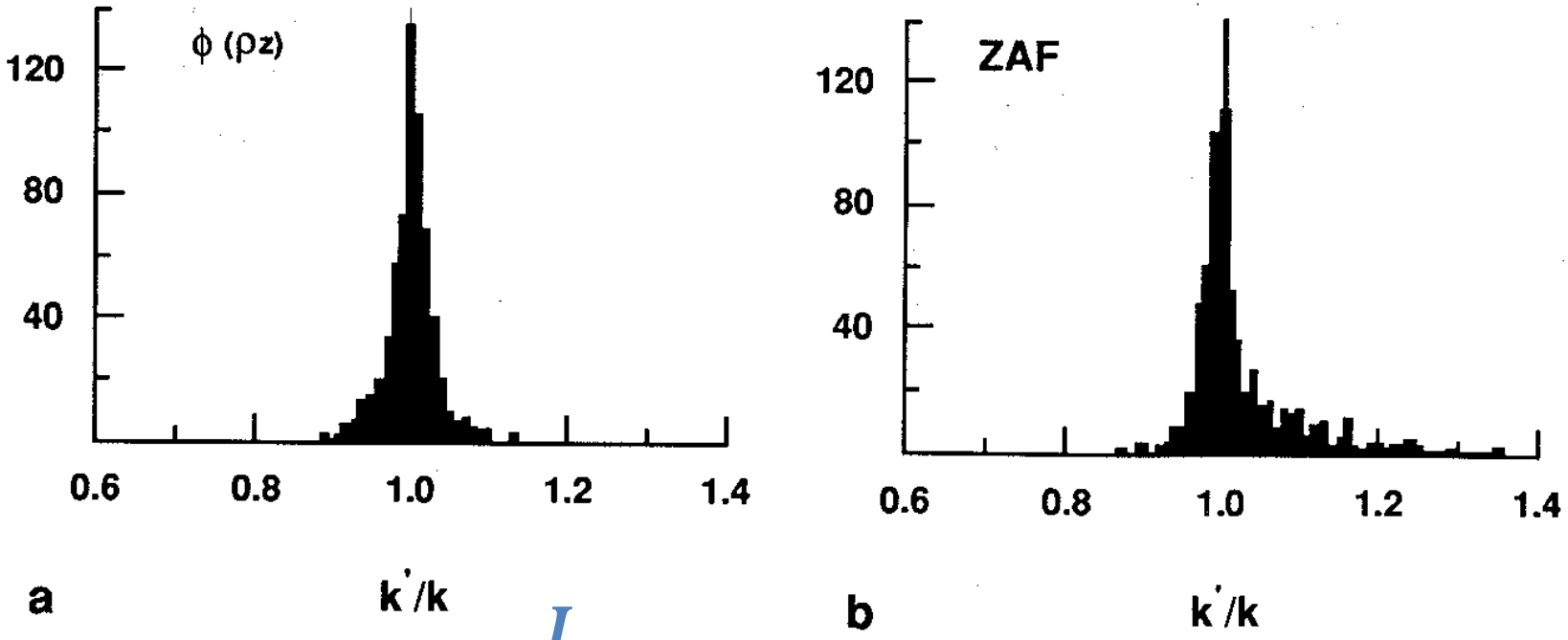

$$K_i = \frac{I_i}{I_{(i)}} \text{ , } K' \text{calculé}, K \text{ mesuré}$$

Comparaison
Pouchou Database (1991)

Procedure	826 Analyses		577 Analyses Effect of Z predominant		242 Analyses Absorption predominant	
	m	*s*	*m*	*s*	*m*	*s*
XPP	0.9997	1.79%	0.9983	1.58%	1.0023	2.17%
PAP	0.9982	1.91%	0.9975	1.60%	0.9993	2.50%
Love-Scott	0.9915	2.59%	0.9941	1.79%	0.9845	3.79%
Tanuma-Nagashima	0.9917	2.73%	0.9893	2.05%	0.9967	3.85%
Bastin 861	1.0090	2.92%	1.0138	2.84%	0.9976	2.83%
ZAF f(x) Heinrich	0.9850	2.74%	0.9881	2.01%	0.9765	3.84%
ZAF Philibert simpl.	0.9999	4.05%	0.9854	1.96%	1.0339	5.50%
ZAF Ruste-Zeller	1.0089	4.21%	0.9958	2.02%	1.0401	6.07%
Win X-Ray	**1.002**	**2.74%**	**0.99**	**2.62%**	**1.01**	**2.69%**

Comparaison
Pouchou Database (1991) Borures

Procedure	μ/ρ	k(calculated)/k(experimental) Ave.	Standard Deviation
PAP	P	1.0075	3.95
XPP	P	1.0106	4.76
Bastin 861	B	1.0080	5.17
Bastin 861	P	1.0162	6.25
ZAF Ruste-Zeller	P	1.0139	9.59
Love-Scott quadrilateral	P	1.0148	12.24
ZAF+$f(\chi)$ Heinrich	P	1.0657	14.25
Tanuma-Nagashima	P	1.1018	17.51
ZAF Philibert simplified	P	1.1433	19.72

Win X-Ray **0.999** **1.77%**

MC X-Ray: Complex Geometries

https://www.memrg.com/programs-download

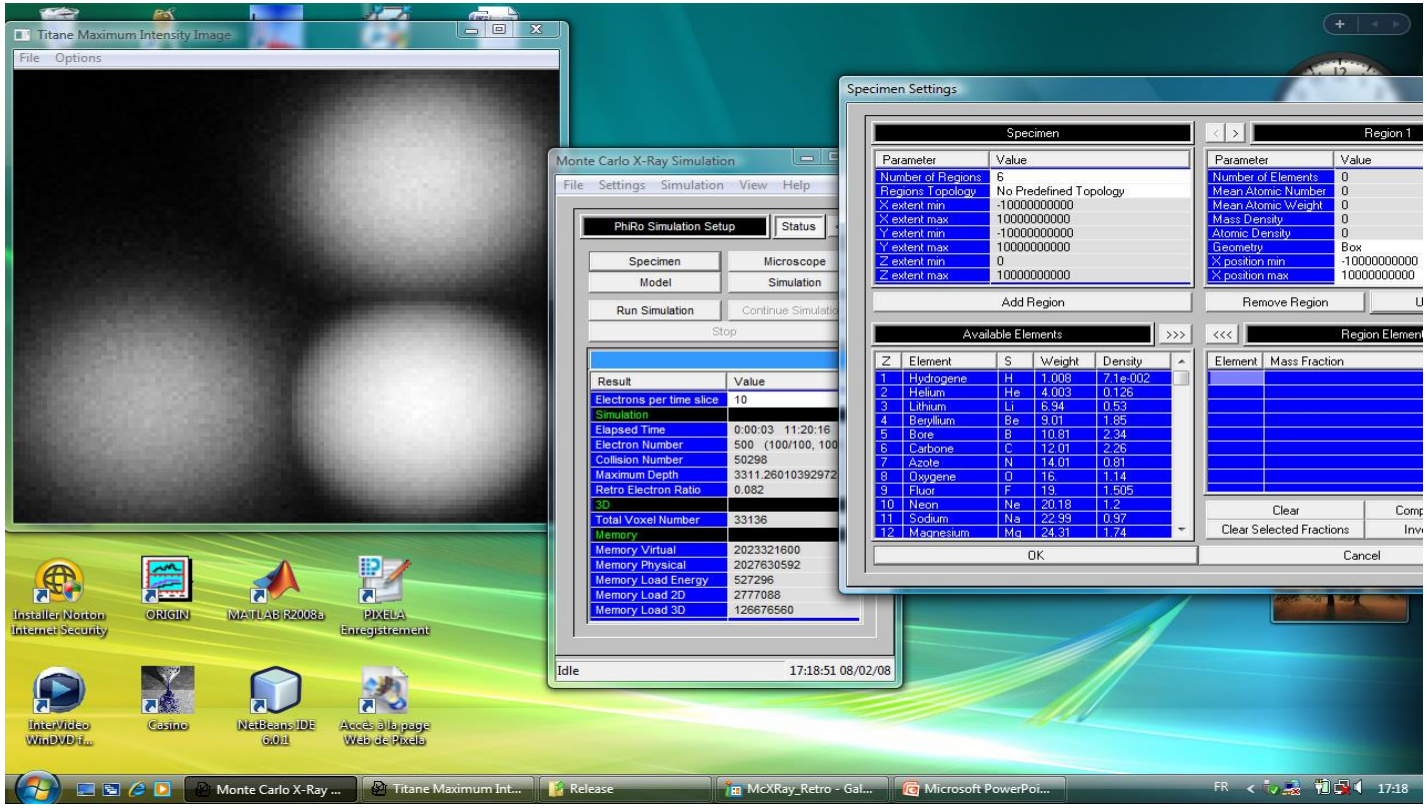

488
doi: 10.1017/S1431927609092423

Microsc Microanal 15(Suppl 2), 2009

MC X-Ray, a New Monte Carlo Program for Quantitative X-Ray Microanalysis of Real Materials

Raynald Gauvin and Pierre Michaud

Sphère de 1 µm de W sur C, 20 keV, 40° TOA

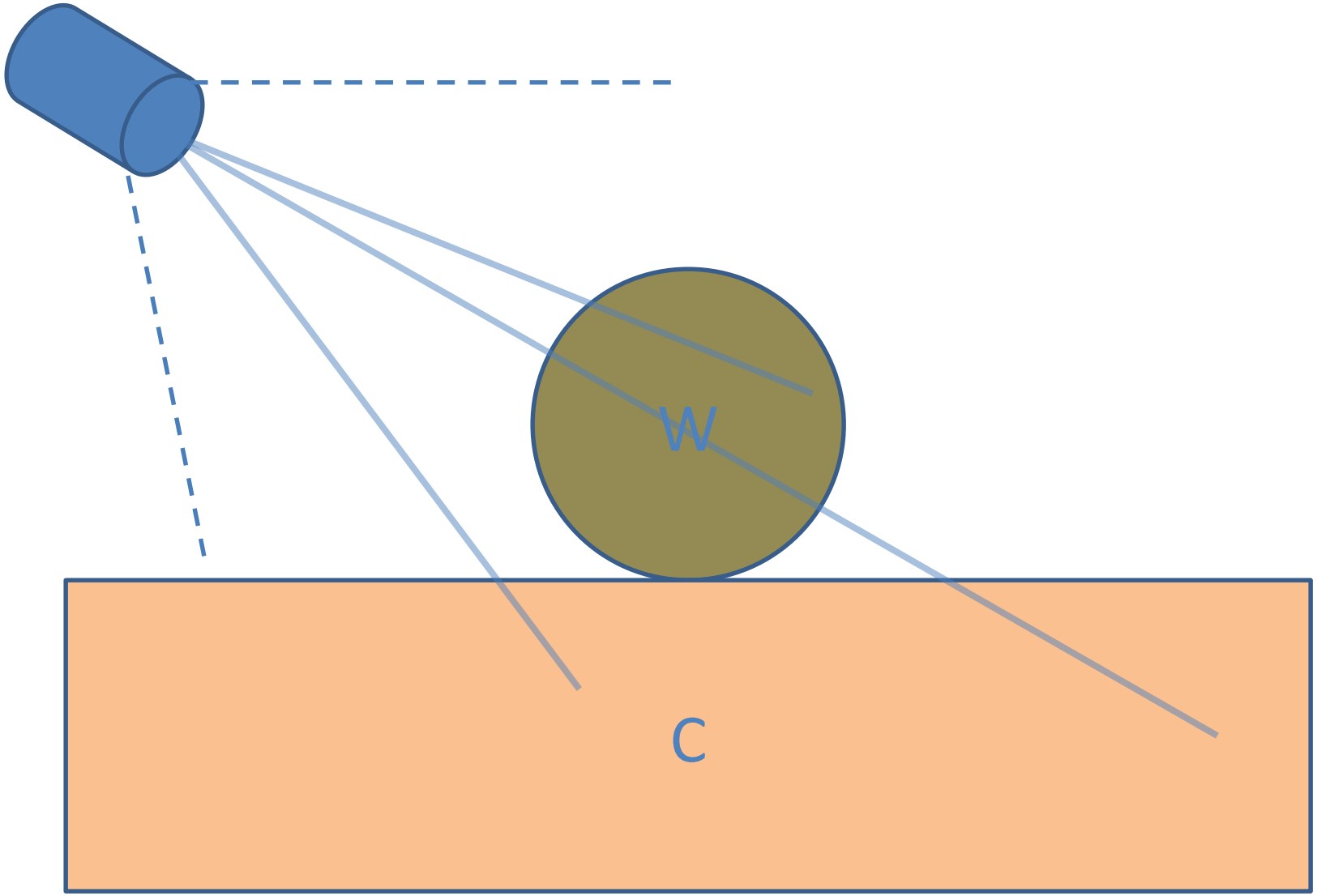

Sphère de 1 µm de W sur C, 20 keV, 40° TOA

C Kα

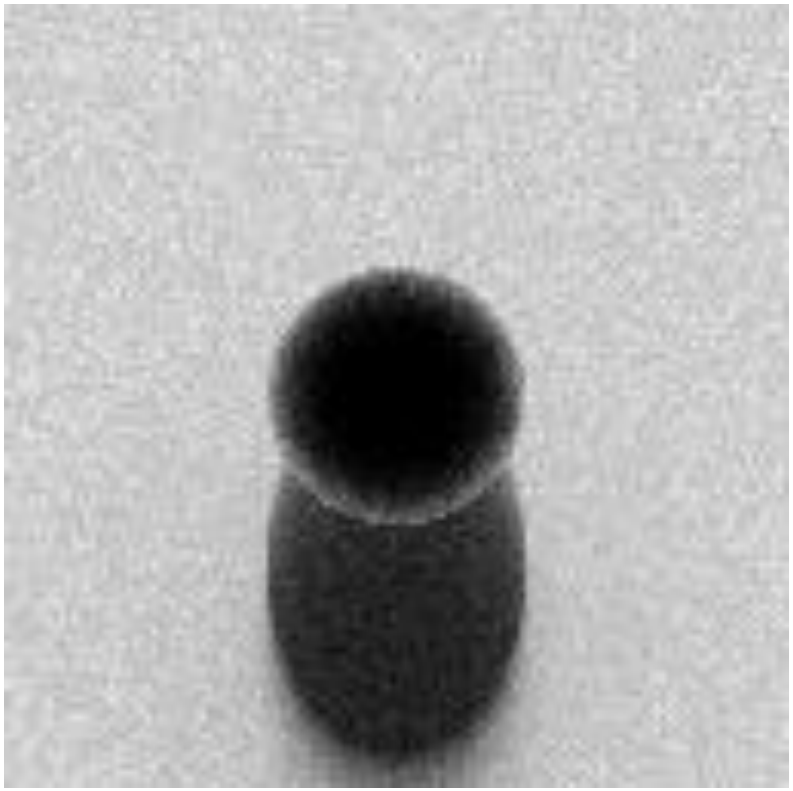

W Mα

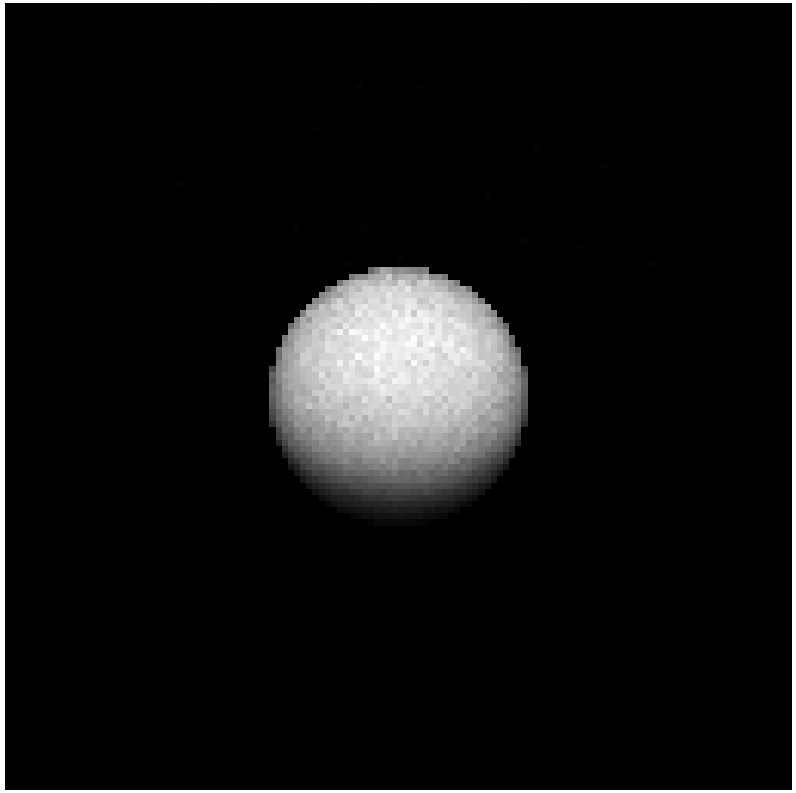

Received: 28 October 2024 | Revised: 27 June 2025 | Accepted: 22 July 2025

DOI: 10.1111/jmi.70018

Journal of Microscopy RMS

ORIGINAL ARTICLE

Comparison of two Monte Carlo approaches for homogeneous bulk samples

Dawei Gao | Yu Yuan | Nicolas Brodusch | Raynald Gauvin

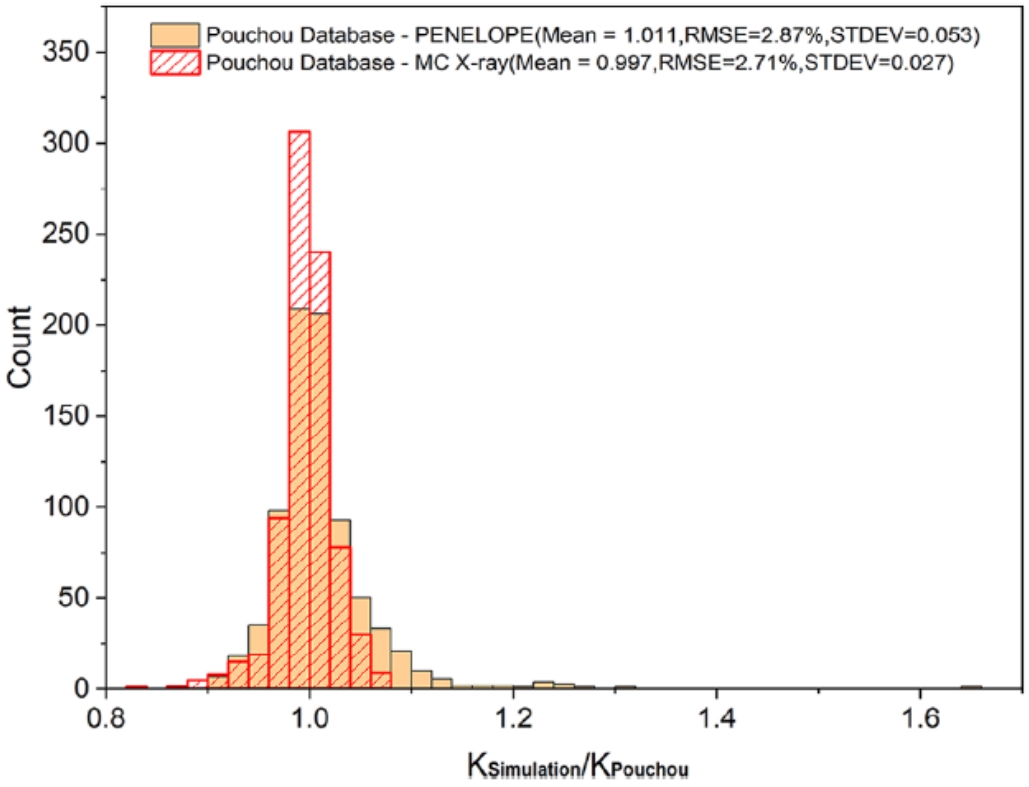

Pouchou Data Base

	Mean	Rms (%)
MC X-Ray	0.997	2.71
PENELOPE	1.011	2.87

Microscopes Électroniques en Balayage à Cathode Froide. Gauvin's Group.

Hitachi SU-8000 (2010)

0.5 nm at 30 keV
2 nm at 0.2 keV

Hitachi SU-8230 (2014)

0.4 nm at 30 keV,
1.8 nm at 0.2 keV

MgO sur substrat de Al

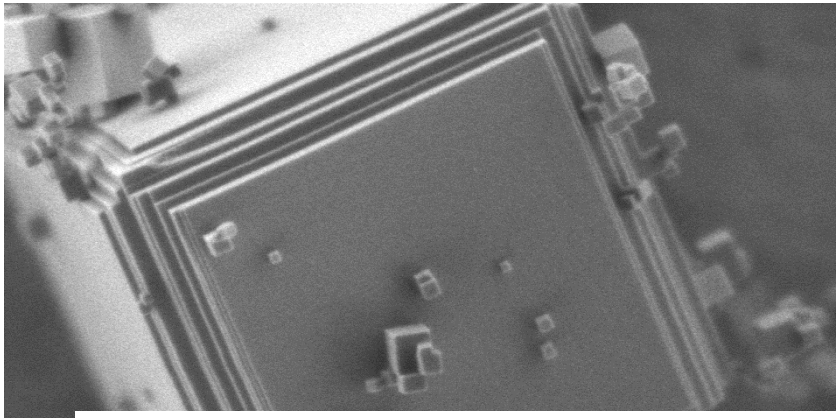

pper detector

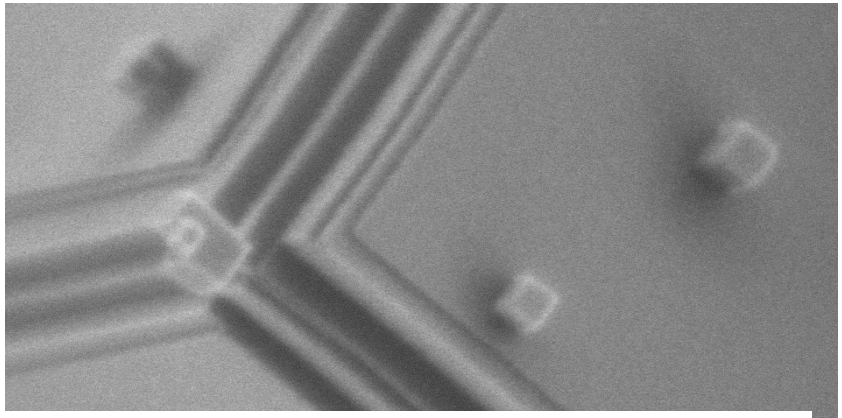

Cold-FEG, Meilleure Résolution Spatiale

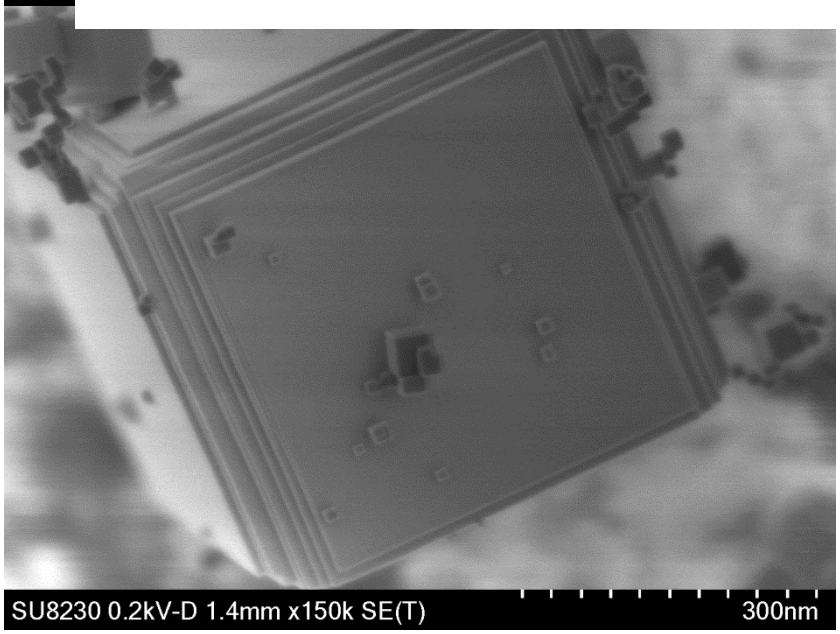

Top detector

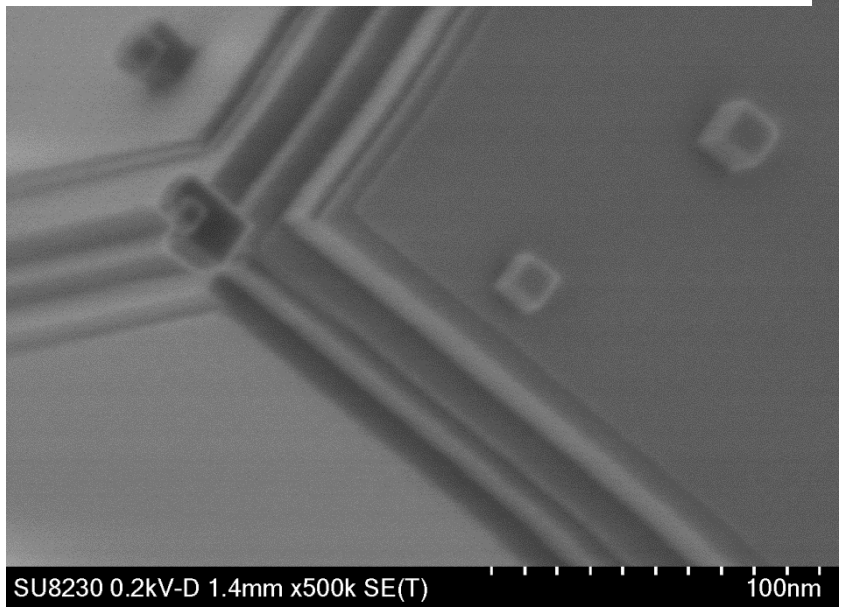

MICROSCOPY RESEARCH AND TECHNIQUE 78:30–39 (2015)

Electron Backscatter Diffraction Applied to Lithium Sheets Prepared by Broad Ion Beam Milling

NICOLAS BRODUSCH,[1]* KARIM ZAGHIB,[2] AND RAYNALD GAUVIN[1]
[1]*Mining and Materials Engineering Department, McGill University, Montréal, Québec, Canada*
[2]*Institut de Recherche d'Hydro-Québec, Varennes, Québec, Canada*

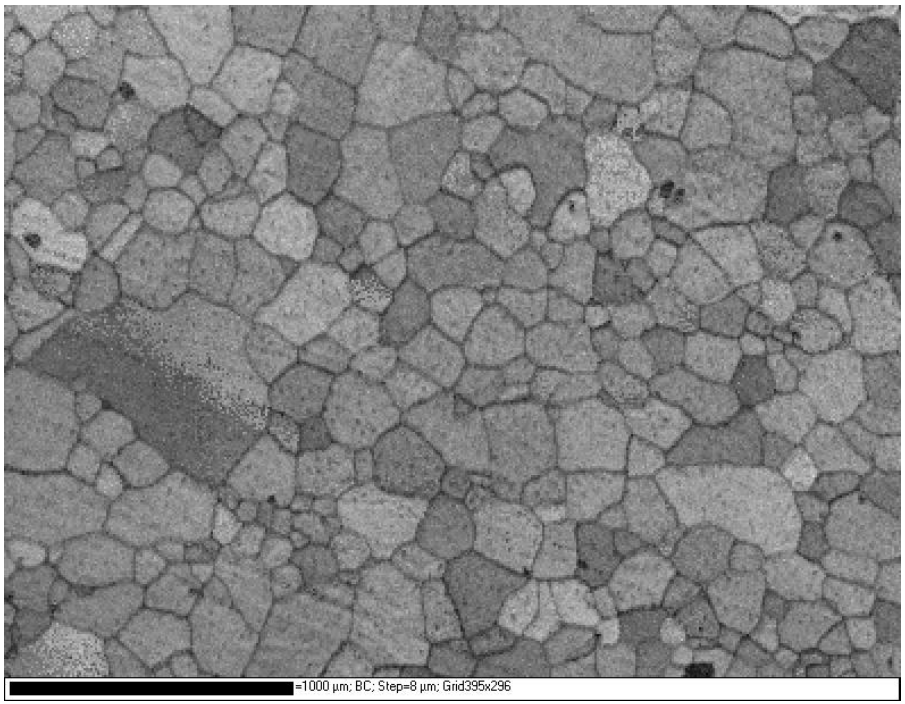

Band contrast map

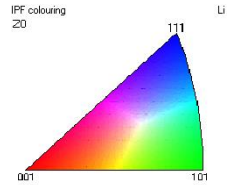

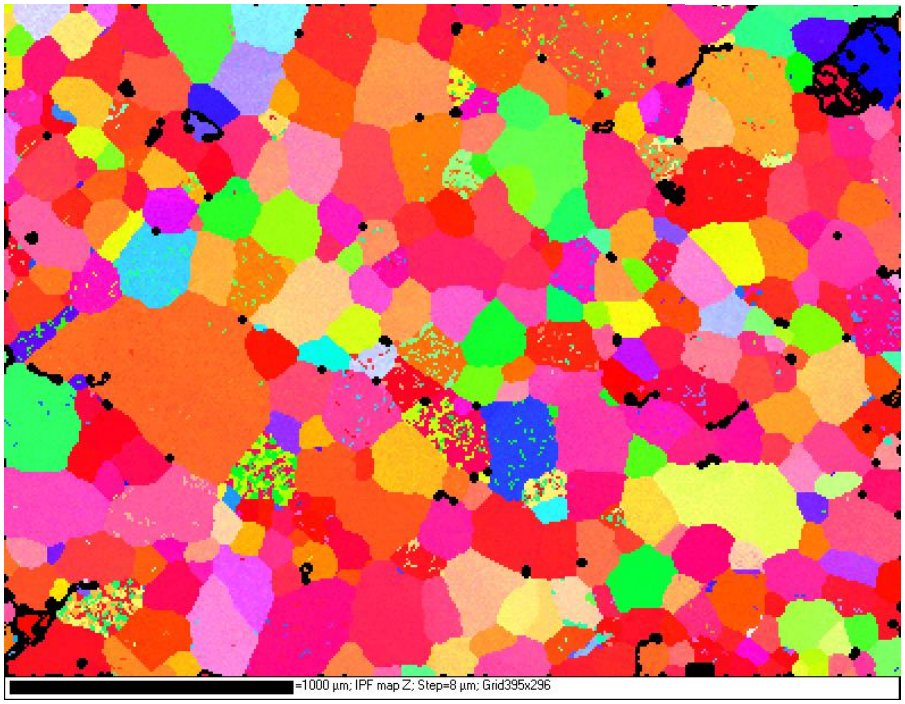

Inverse pole figure map

X-Max

400000 cps @ 80 mm2

In practice

Detector area	20mm²	50mm²	80mm²
Resolution (eV):			
MnK_α resolution	129	129	129
Operating angle	0° to 45°		
Temperature range	10°C to 30°C		
Altitude	Sea level to 1,500m		

Alliage Mg – Al – Ca
3 keV EDS, SU 8000, Oxford X-Max 80

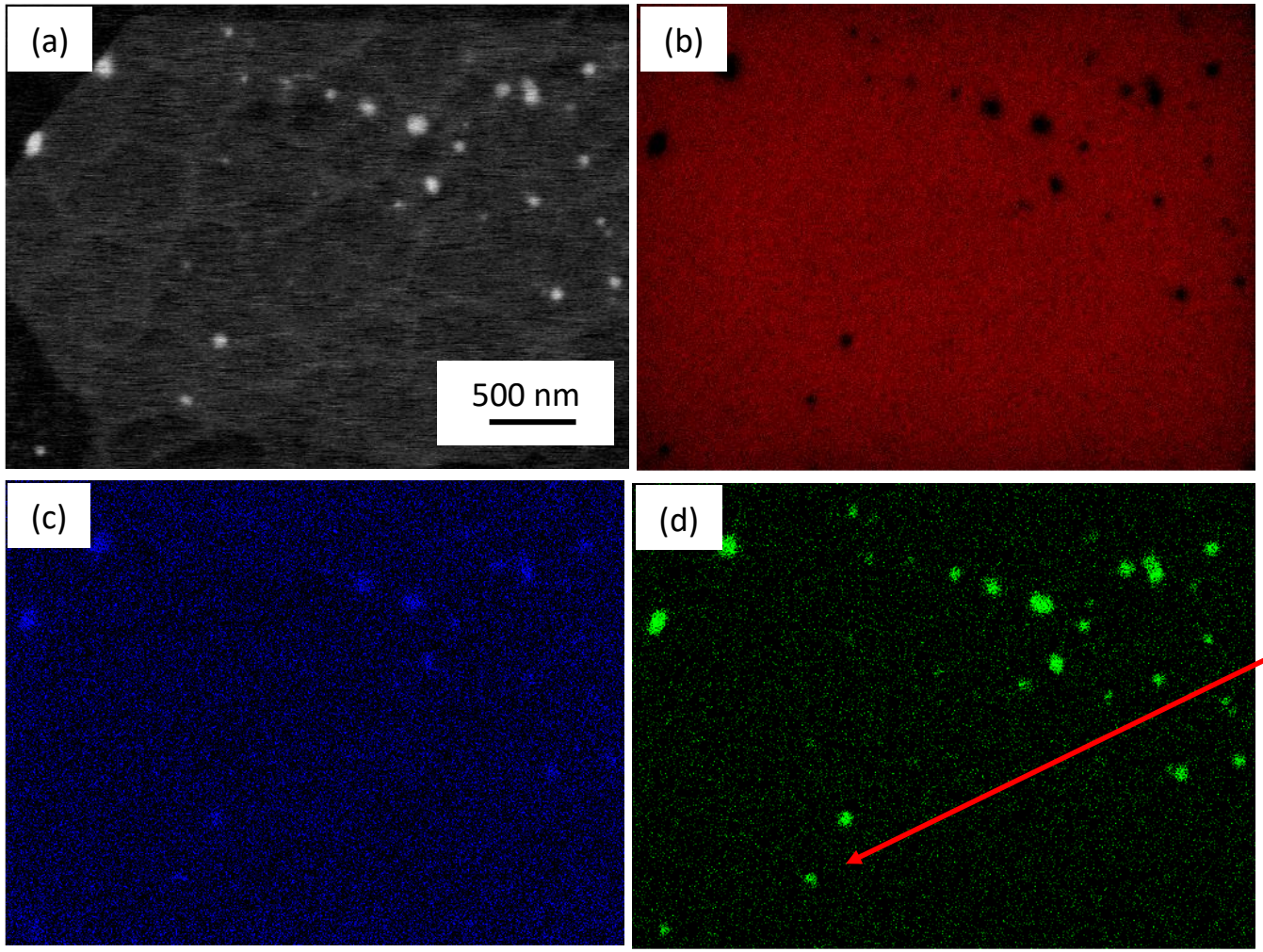

Figure 7. (a) SEM-BSE image, (b) Mg, (c) Al and (Ca) X-ray maps

Courant de faisceau vs Temps

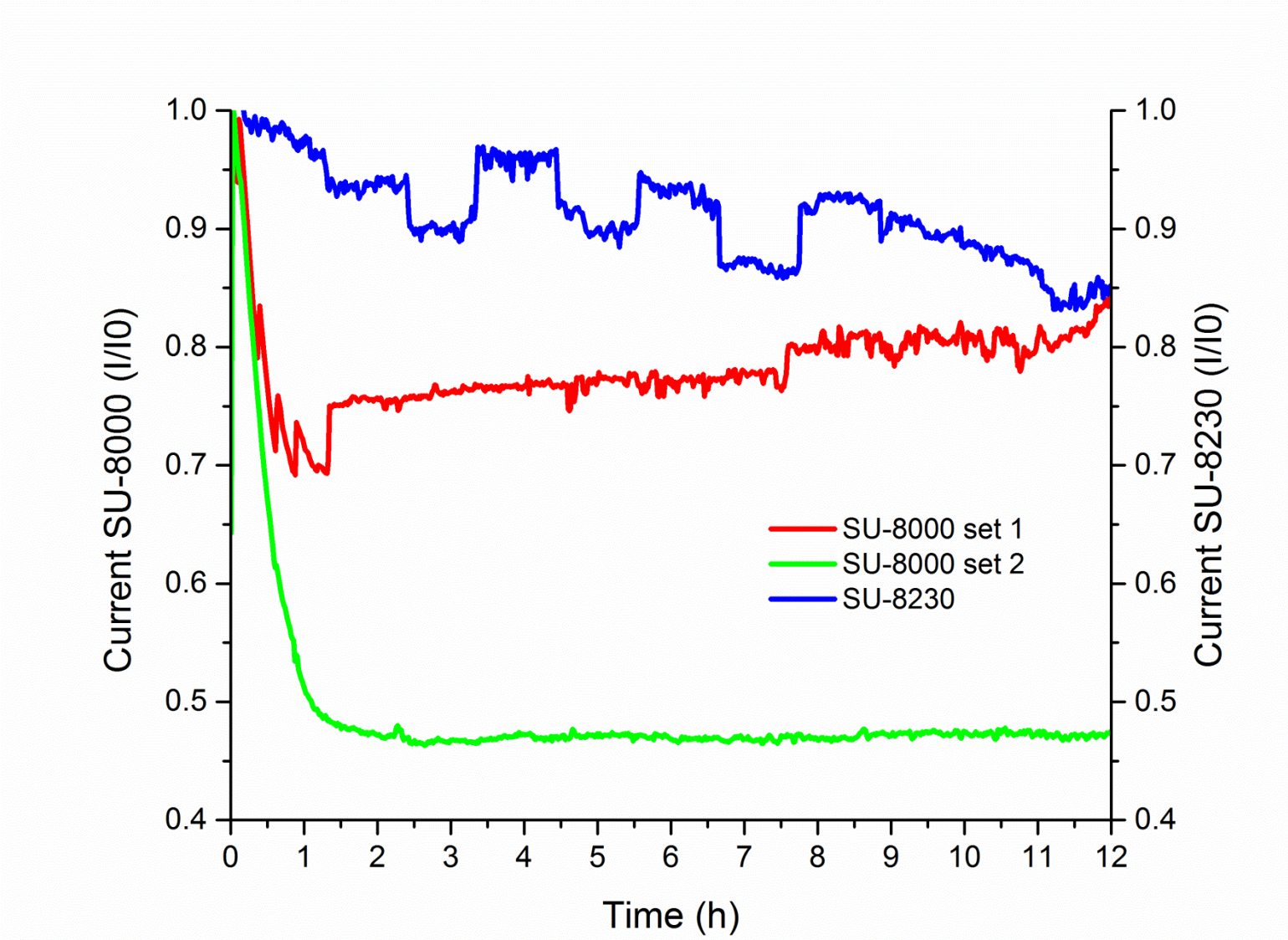

Microanalyse des Films Minces Sans Absorption et Fluorescence

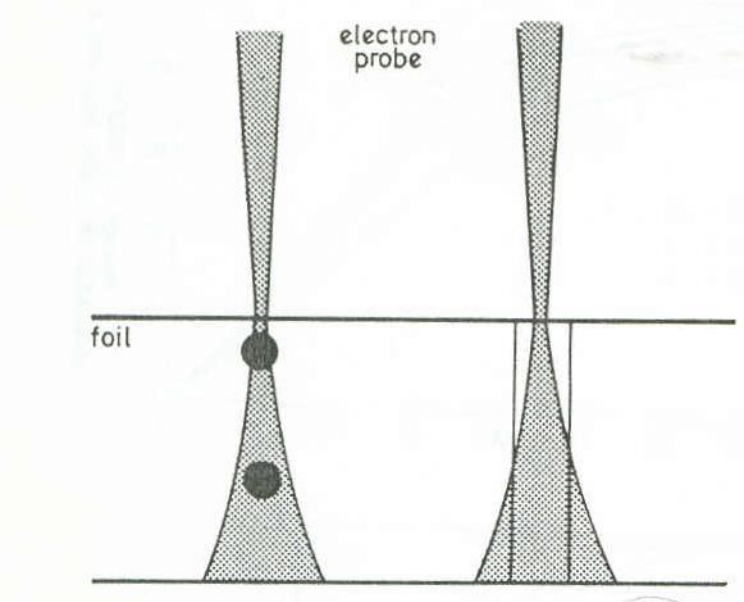

$$I_A = \left(\frac{\Omega}{4\pi}\right) D_e \frac{Q_A \varpi_A \alpha_A \varepsilon_A}{A_A} N_0 \rho t C_A$$

$$D_e = \frac{it^*}{e}$$

Cliff et Lorimer (1975)

$$\frac{C_A}{C_B} = K_{AB}\frac{I_A}{I_B}$$

$$C_A + C_B = 1$$

Pas de besoin de mesurer le courant.
Pas de besoin de mesurer l'épaisseur si l'absorption est négligeable.
K_{AB} mesuré expérimentalement.

Goldstein, Costley, Lorimer et Reed (1977)

$$K_{AB} = \frac{Q_B \varpi_B \alpha_B \varepsilon_B A_A}{Q_A \varpi_A \alpha_A \varepsilon_A A_B}$$

Les facteurs K_{AB} mesurés expérimentalement sont beaucoup plus précis que ceux calculés.

La méthode des f ratios

$$f_A = \frac{I_A}{I_A + I_B}$$

Microsc. Microanal. 16, 821–830, 2010
doi:10.1017/S1431927610094018

Microscopy AND Microanalysis

Development of a New Quantitative X-Ray Microanalysis Method for Electron Microscopy

Paula Horny,[1,2,*] Eric Lifshin,[3] Helen Campbell,[1] and Raynald Gauvin[1]

[1]*Department of Mining and Materials Engineering, McGill University, 3610 University Street, Montréal, Québec H3A 2B2, Canada*
[2]*Département de Génie des Mines, de la Métallurgie et des Matériaux, Université Laval, Québec G1K 7P4, Canada*
[3]*College of Nanoscale Science and Engineering, University at Albany—State University of New York, 251 Fuller Road, Albany, NY 12203, USA*

La méthode des f ratios

$$f_A = \frac{I_A}{I_A + I_B}$$

$$f_A = \frac{1}{1 + \Lambda_{A-B} K_{A-B} \frac{\int \varphi_B(\rho z) e^{\chi_B \rho z} d\rho z}{\int \varphi_A(\rho z) e^{\chi_A \rho z} d\rho z} \frac{F_B}{F_A} \frac{c_B}{c_A}}$$

P. Horny, E. Lifshin, H. Campbell and R. Gauvin (2010), “Development of a New Quantitative X-Ray Microanalysis Method for Electron Microscopy”, Microscopy & Microanalysis, Vol. 16, No. 6, pp. 821-830.

La méthode des f ratios

Microsc. Microanal. 18, 915–940, 2012
doi:10.1017/S1431927612001468

Microscopy AND Microanalysis

REVIEW ARTICLE

What Remains to Be Done to Allow Quantitative X-Ray Microanalysis Performed with EDS to Become a True Characterization Technique?

Raynald Gauvin*

f ratios

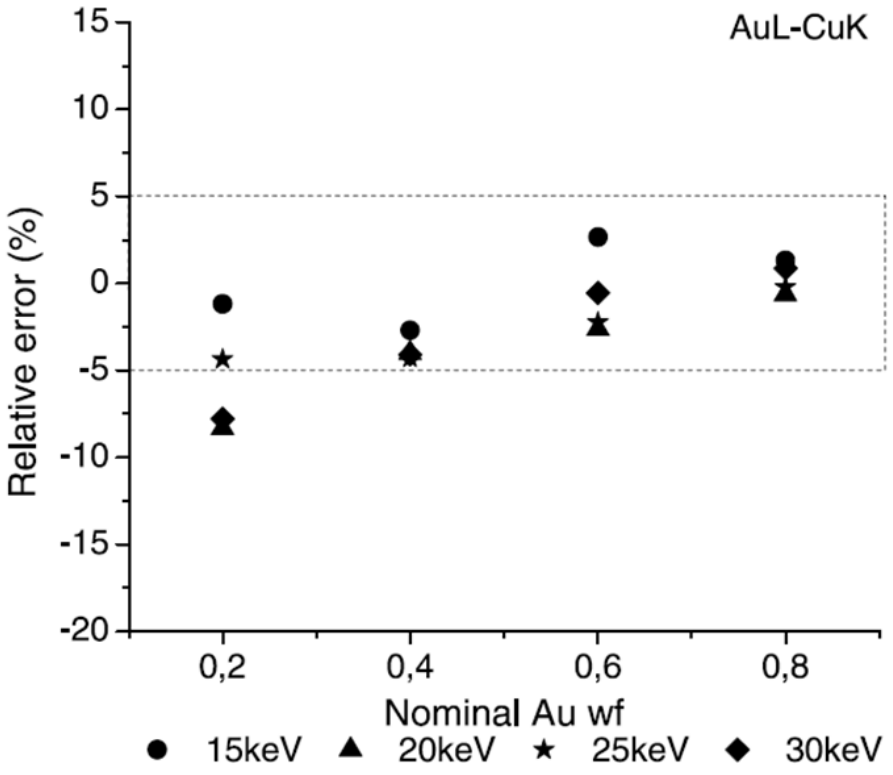

Standardless

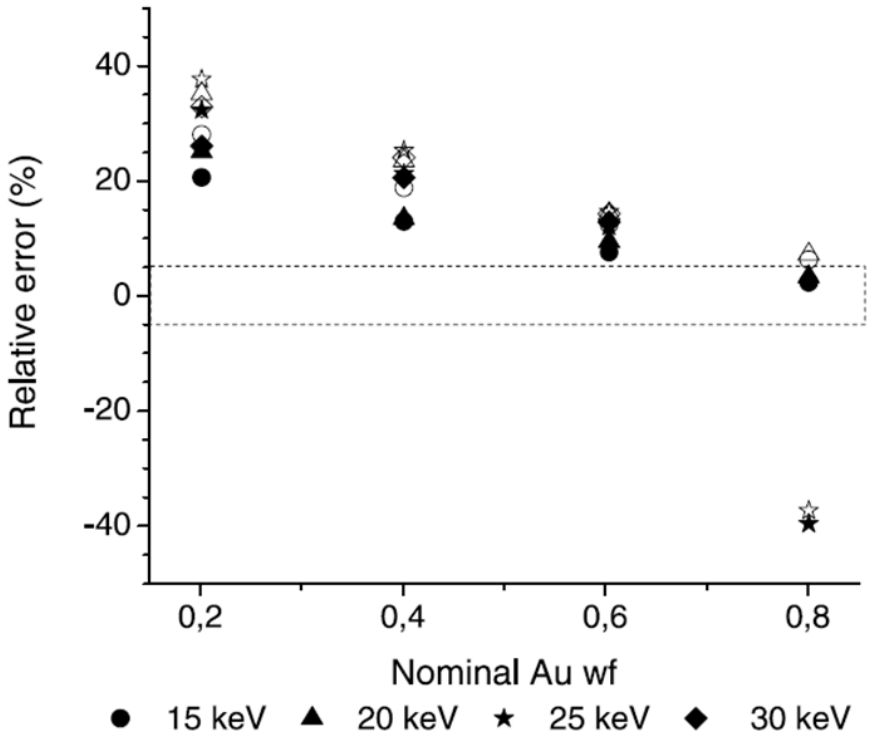

P. Horny, E. Lifshin, H. Campbell and R. Gauvin (2010), "Development of a New Quantitative X-Ray Microanalysis Method for Electron Microscopy", Microscopy & Microanalysis, Vol. 16, No. 6, pp. 821-830.

La méthode des f ratios

$$f_A = \frac{I_A}{I_A + I_B}$$

$$f_A = \frac{1}{1 + \frac{I_B}{I_A}} = \frac{1}{1 + K_{AB}\frac{C_B}{C_A}}$$

$$1 + K_{AB}\frac{C_B}{C_A} = 1 + \frac{I_B}{I_A}$$

$$\frac{C_A}{C_B} = K_{AB}\frac{I_A}{I_B}$$

Couple de diffusion Mg – Al

415 ^{o}C, 240 h

Mg **γ – $Al_{12}Mg_{17}$** **β – Al_3Mg_2** **Fe in Al** **Al**

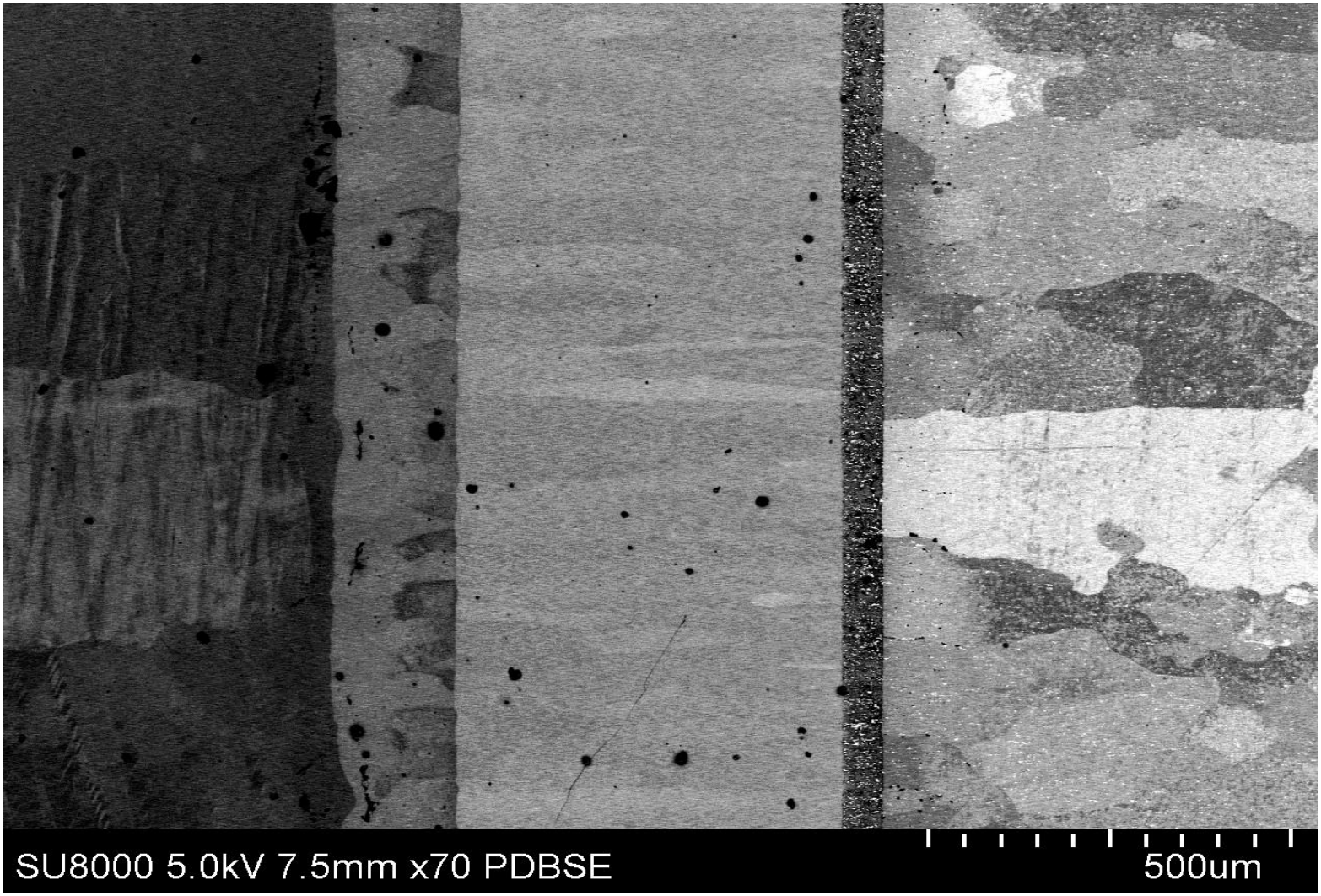

Calculs des f ratios avec un facteur de correction Λ_{Mg-Al}

$$f_{Mg} = \frac{(I_{Mg})^S}{(I_{Mg})^S + \Lambda_{Mg-Al}(I_{Al})^S}$$

Détermination du facteur de Calibration

$$f_{Mg-Al} = \frac{I_{Mg}}{I_{Mg} + I_{Al}}$$

$$\Lambda_{Mg-Al} = \left(\frac{1 - f_{Mg-Al}}{f_{Mg-Al}}\right)^{M} \left(\frac{f_{Mg-Al}}{1 - f_{Mg-Al}}\right)^{S}$$

Mesure du facteur de calibration

- Un alliage 36% Mg – 64 % a été coulé à McGill.
- La composition a été déterminée par spectroscopie d'émission atomique par plasma à couplage inductif (ICPAS-AES)
- L'homogénéité de l'échantillon a été testée par des spectres de rayons X obtenus à différents endroits sur l'échantillon poli.

E_0 (keV)	$\Lambda_{Mg\text{-}Al}$
5	1.057
30	1.026

$$\Delta C = \frac{\partial C}{\partial f}\Delta f$$

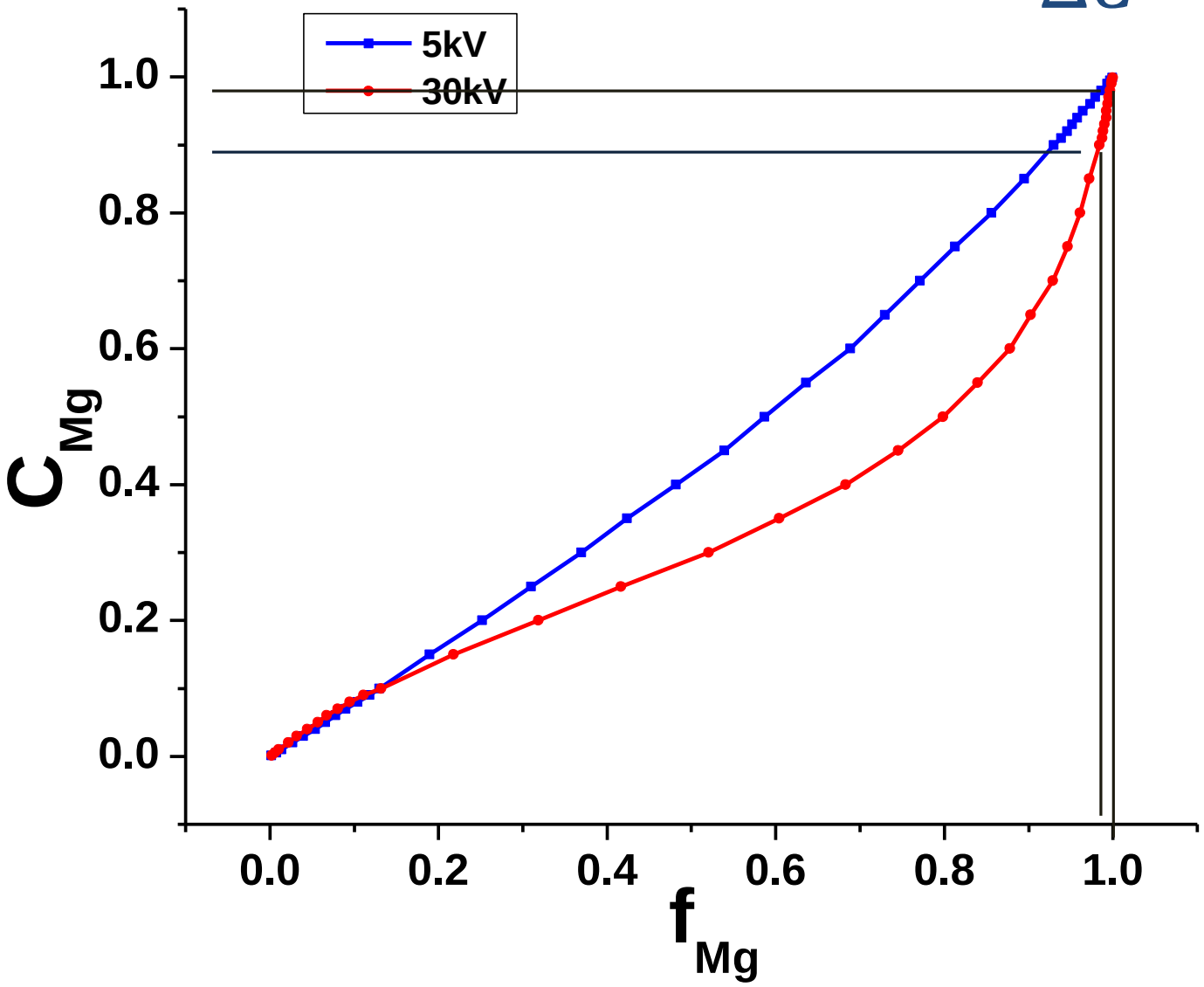

Courbe de callibration pour c_{Mg}

$$c_{Mg} = af_{Mg}^6 + bf_{Mg}^5 + cf_{Mg}^4 + df_{Mg}^3 + ef_{Mg}^2 + hf_{Mg}$$

E_0 (keV)	a	b	c	d	e	h	R^2
5	1.987	-5.4594	5.9389	-2.6802	0.3693	0.8463	1
30	22.028	-54.858	49.618	-18.45	1.8496	0.8038	0.9997

$$C_{Al} = 1 - C_{Mg}$$

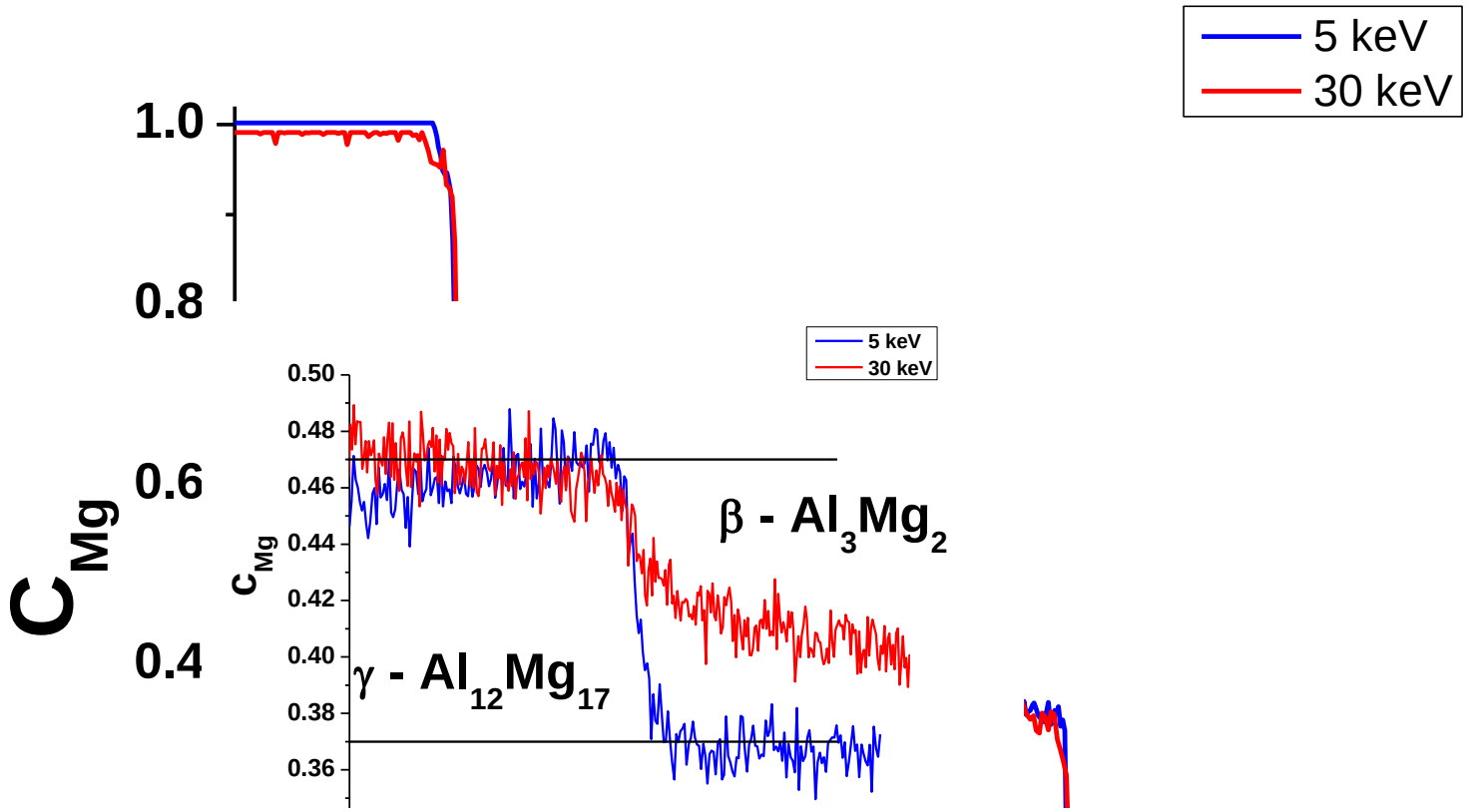

5 keV, correction d'absorption minime, la Fluorescence est négligeable

R. Gauvin et al. Defect and Diffusion Forum Vols. 323-325 (2012) pp. 61-67

Coefficients interdiffusion Al-Mg 415 ^{o}C

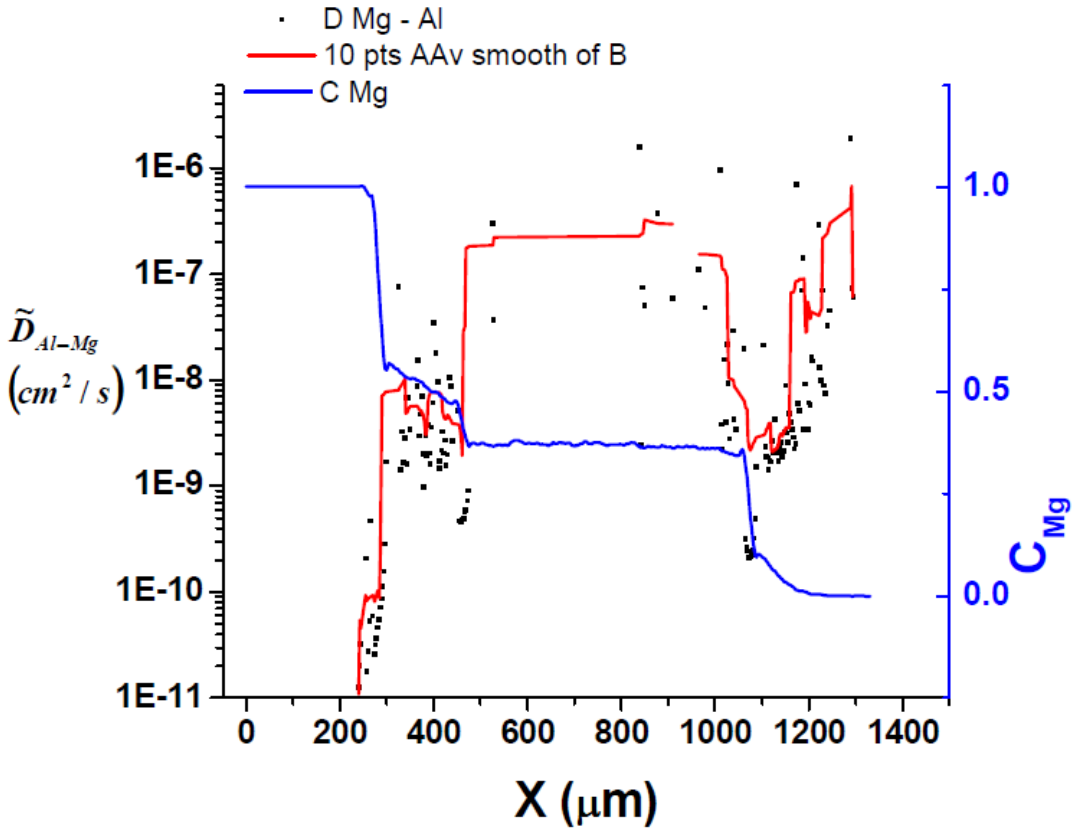

Defect and Diffusion Forum Vols 323-325 (2012) pp 61-67
© (2012) Trans Tech Publications, Switzerland
doi:10.4028/www.scientific.net/DDF.323-325.61

Online: 2012-04-12

Determination of Diffusion Coefficients with Quantitative X- Ray Microanalysis at High – Spatial Resolution

Raynald Gauvin[1, a], Nicolas Brodusch[1,b] and Pierre Michaud[1,c]

Généralisation de la méthode

$$f_i = \frac{I_i}{\sum_{j=1}^{n} I_j}$$

$$f_i = \frac{1}{\sum_{j=1}^{n} F_{ji} \frac{c_j}{c_i}}$$

$$F_{ji} = K_{ij} \frac{\gamma_j}{\gamma_i} \frac{(1 + \delta_c + \delta_{BF})_j}{(1 + \delta_c + \delta_{BF})_i}$$

$$K_{ij} = \Lambda_{\mathrm{ij}} \frac{Q_j \omega_j \alpha_j (1 + T_j) \varepsilon_j A_i}{Q_i \omega_i \alpha_i (1 + T_i) \varepsilon_i A_j}$$

$$\gamma_i = \int_0^{t \; or \; \infty} \varphi(\rho z) \, e^{-\left(\sum_{j=1}^{n} c_j \frac{\mu}{\rho}\right]_j^i \right) cosec\psi \rho z} \, d\rho z$$

$$In\ TEM, \varphi(\rho z) \cong 1$$

Diffusion Ternaire Mg-Al-Zn à 325 °C, 800 h
Cartes Quantitatives Standardless

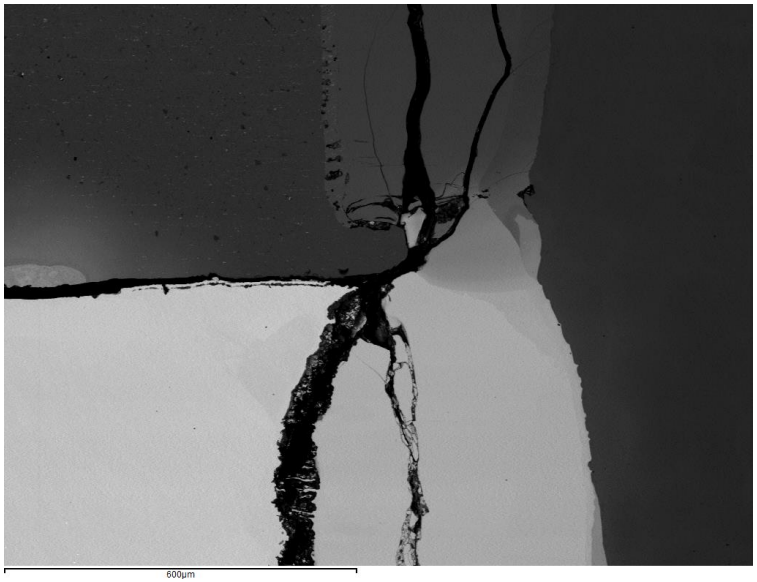

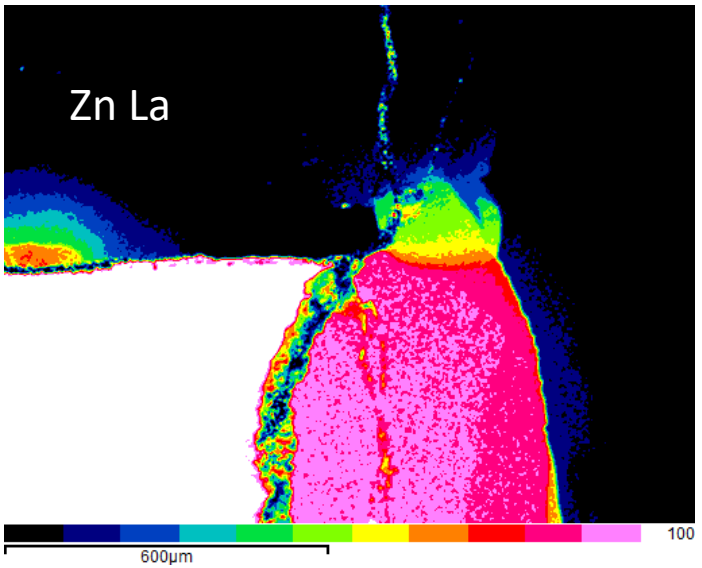

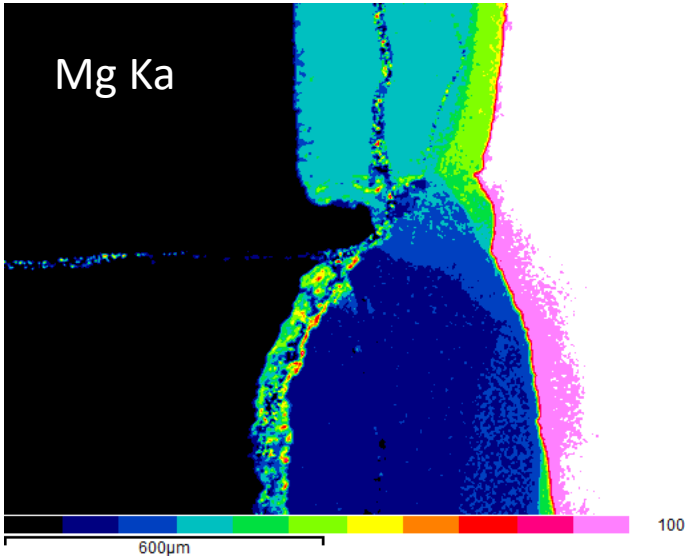

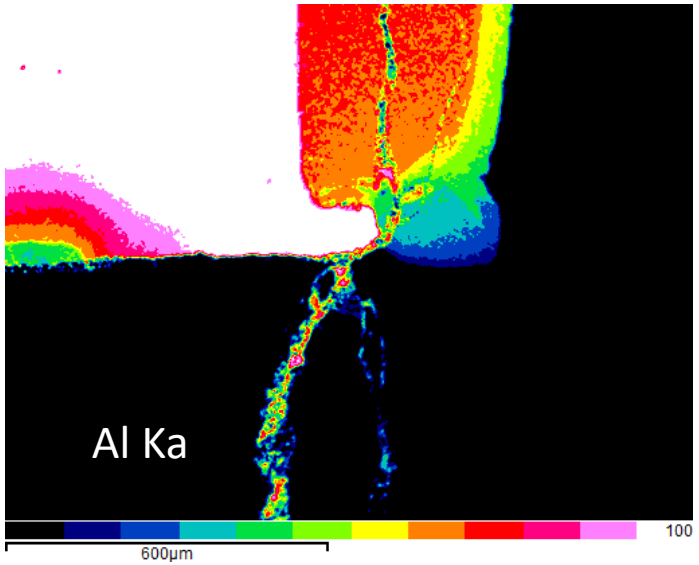

Calcul des f ratios : Ternaires

$$f_{Al-Zn} = \frac{I_{Al}}{I_{Al} + I_{Zn}}$$

$$\Lambda_{Al-Zn} = \left(\frac{1 - f_{Al-Zn}}{f_{Al-Zn}}\right)^{M} \left(\frac{f_{Al-Zn}}{1 - f_{Al-Zn}}\right)^{S}$$

$$\Lambda_{Mg-Al} = \frac{1}{\Lambda_{Al-Mg}} \qquad \Lambda_{Mg-Zn} = \frac{\Lambda_{Al-Zn}}{\Lambda_{Al-Mg}}$$

Calcul avec facteur de correction

$$f_{Al} = \frac{I_{Al}}{I_{Al} + \Lambda_{Al-Mg} I_{Mg} + \Lambda_{Al-Zn} I_{Zn}}$$

$$f_{Mg} = \frac{I_{Mg}}{I_{Mg} + \Lambda_{Mg-Al} I_{Al} + \Lambda_{Mg-Zn} I_{Zn}}$$

Al – Mg – Zn, 5 keV
f Ratios simulés avec MC X-Ray

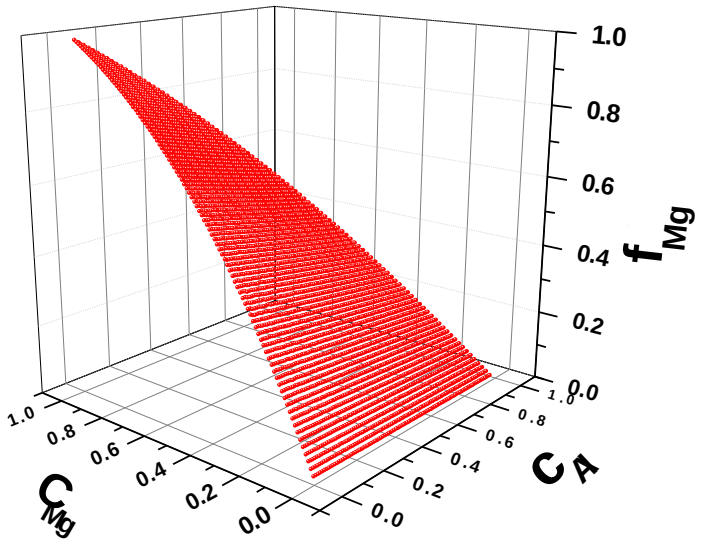

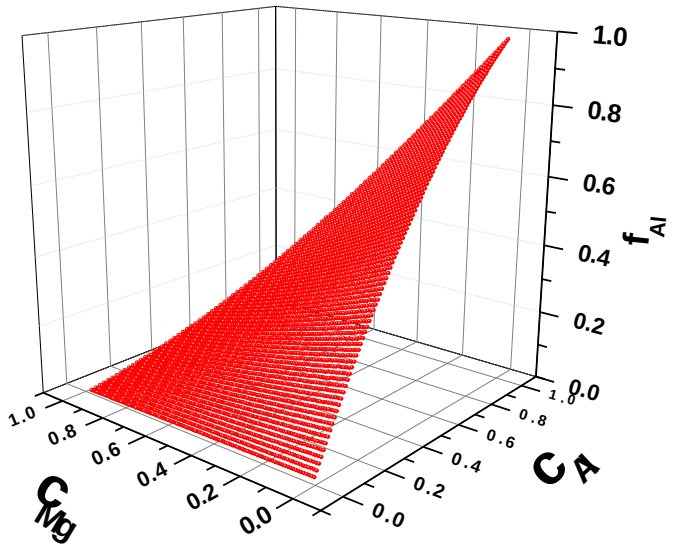

Analyses chimiques quantitatives EDS

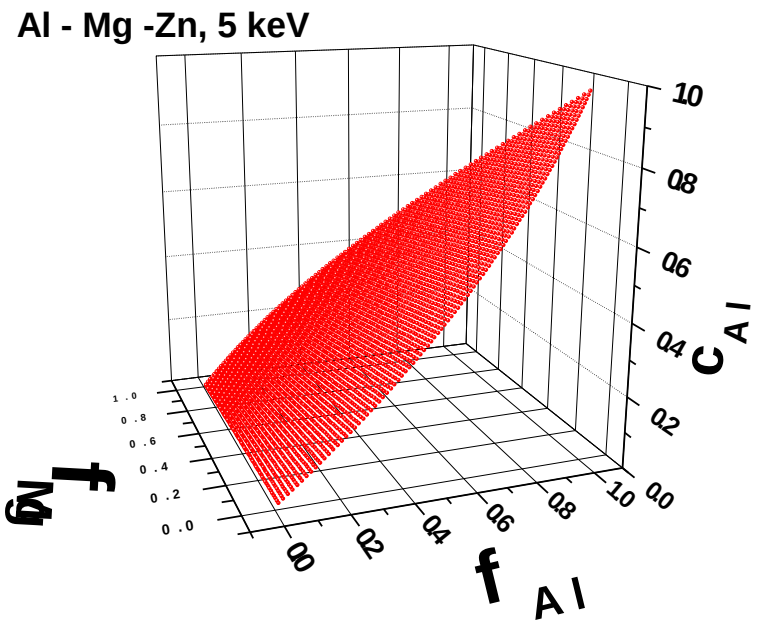

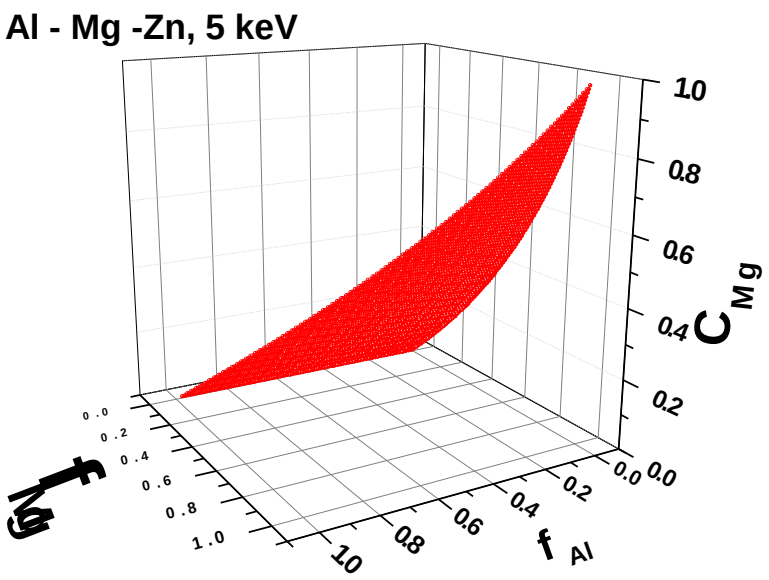

$$C_{Zn} = 1 - C_{Al} - C_{Mg}$$

Carte Al quantitative – 5 keV

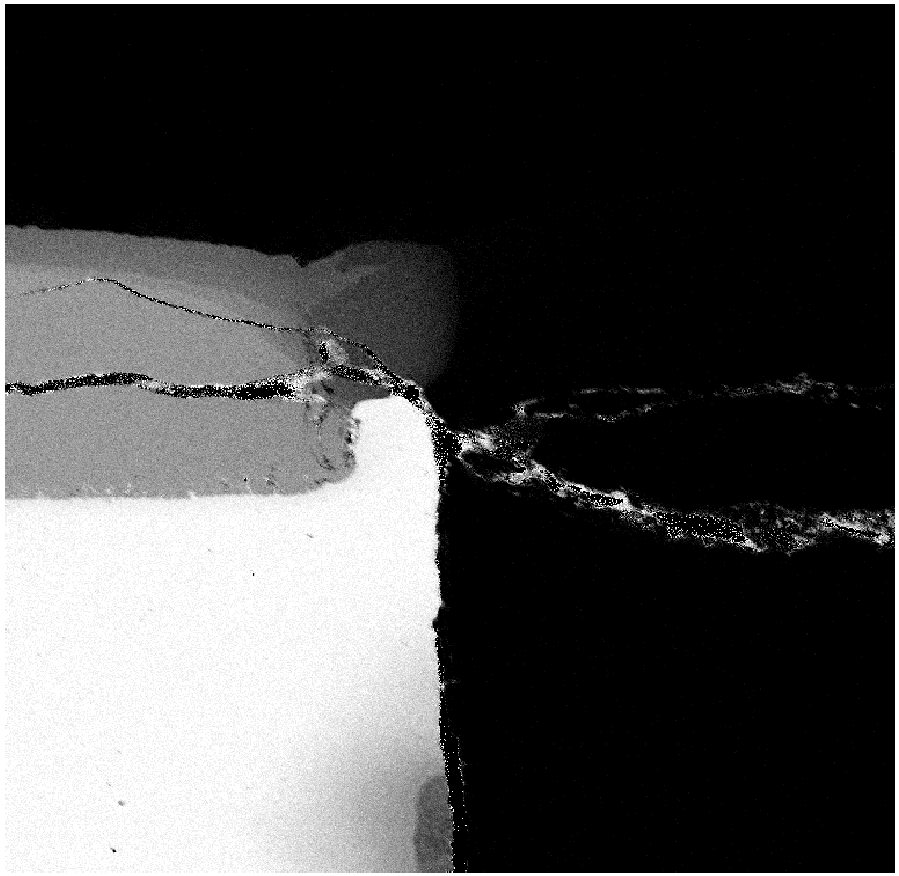

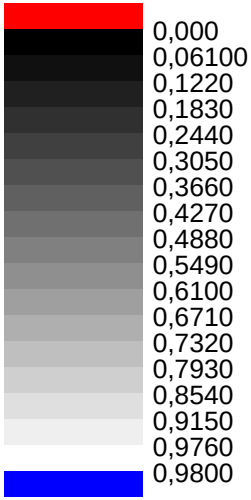

Carte Mg quantitative – 5 keV

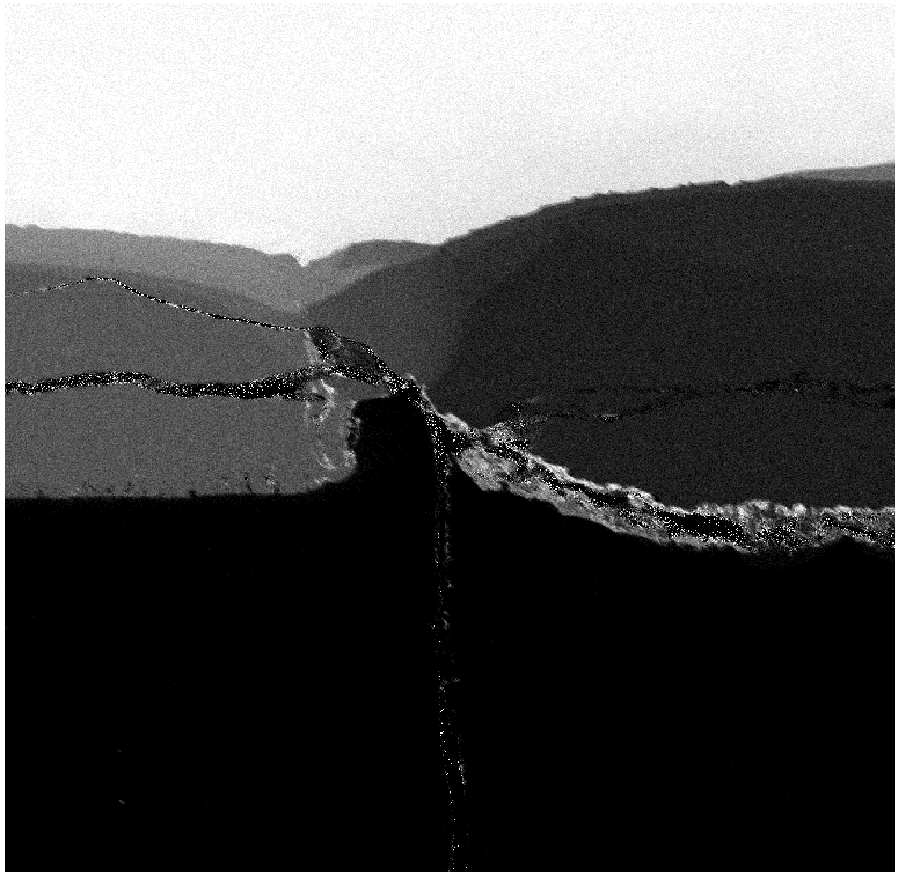

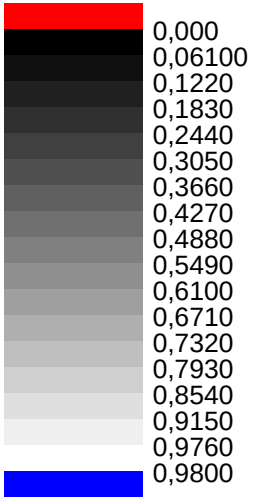

Carte Zn quantitative – 5 keV

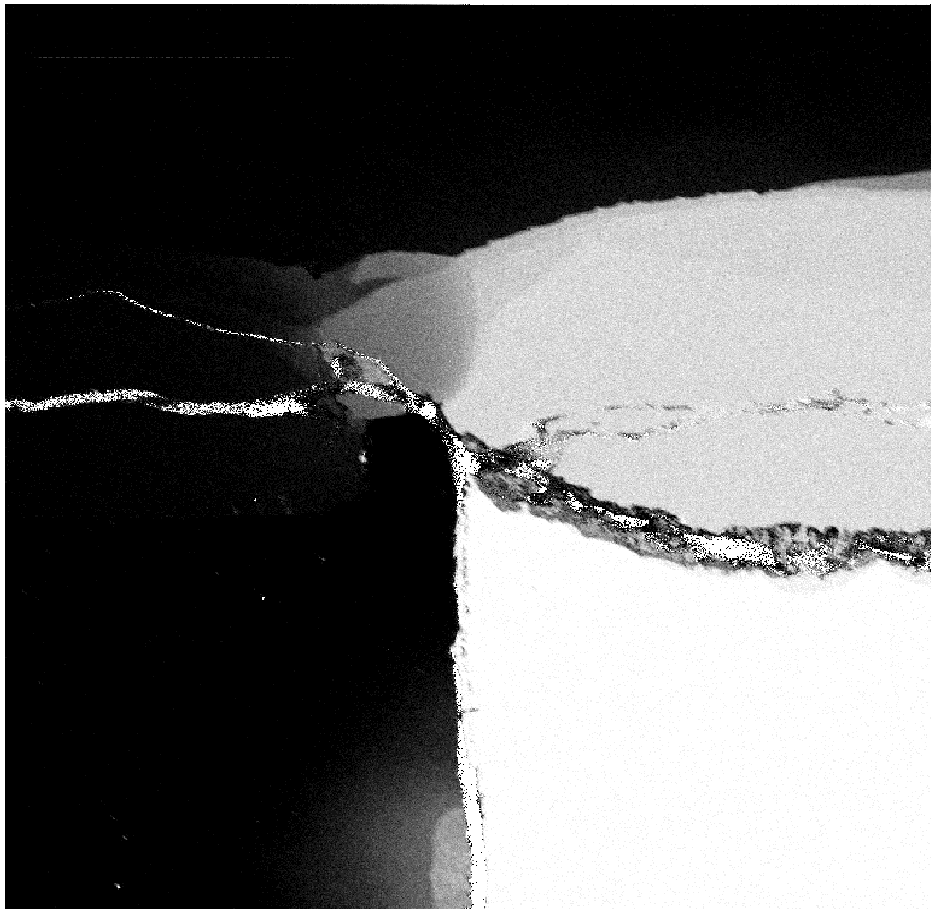

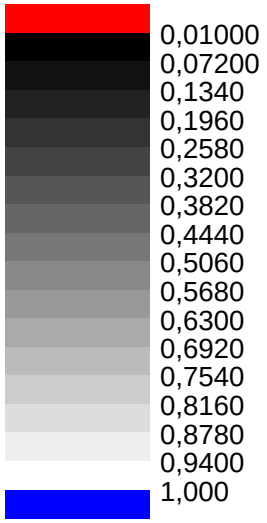

Ternary Phase Diagrams

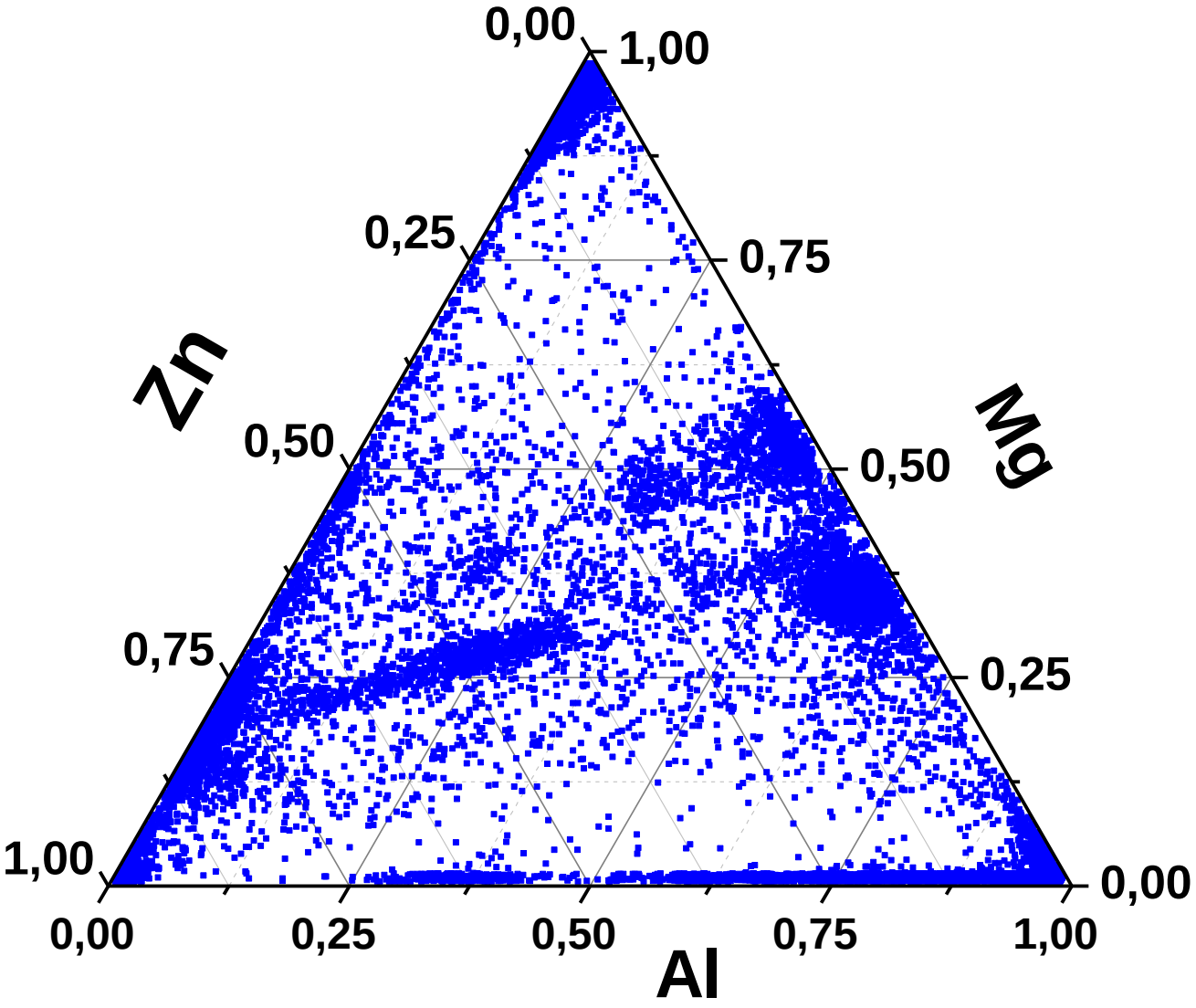

Microscopy and Microanalysis (2019), **25**, 58–69
doi:10.1017/S1431927618015684

Microscopy AND Microanalysis

Original Article

The *f*-Ratio Quantification Method for X-ray Microanalysis Applied to Mg–Al–Zn Alloys

Chaoyi Teng[1]*, Hendrix Demers[2], Xin Chu[1] and Raynald Gauvin[1]

[1]Department of Mining and Materials Engineering, McGill University, Montreal, Quebec, Canada H3A 0C5 and [2]Centre d'excellence en électrification des transports et stockage d'énergie, Hydro-Québec, Varennes, Québec, Canada J3X 1S1

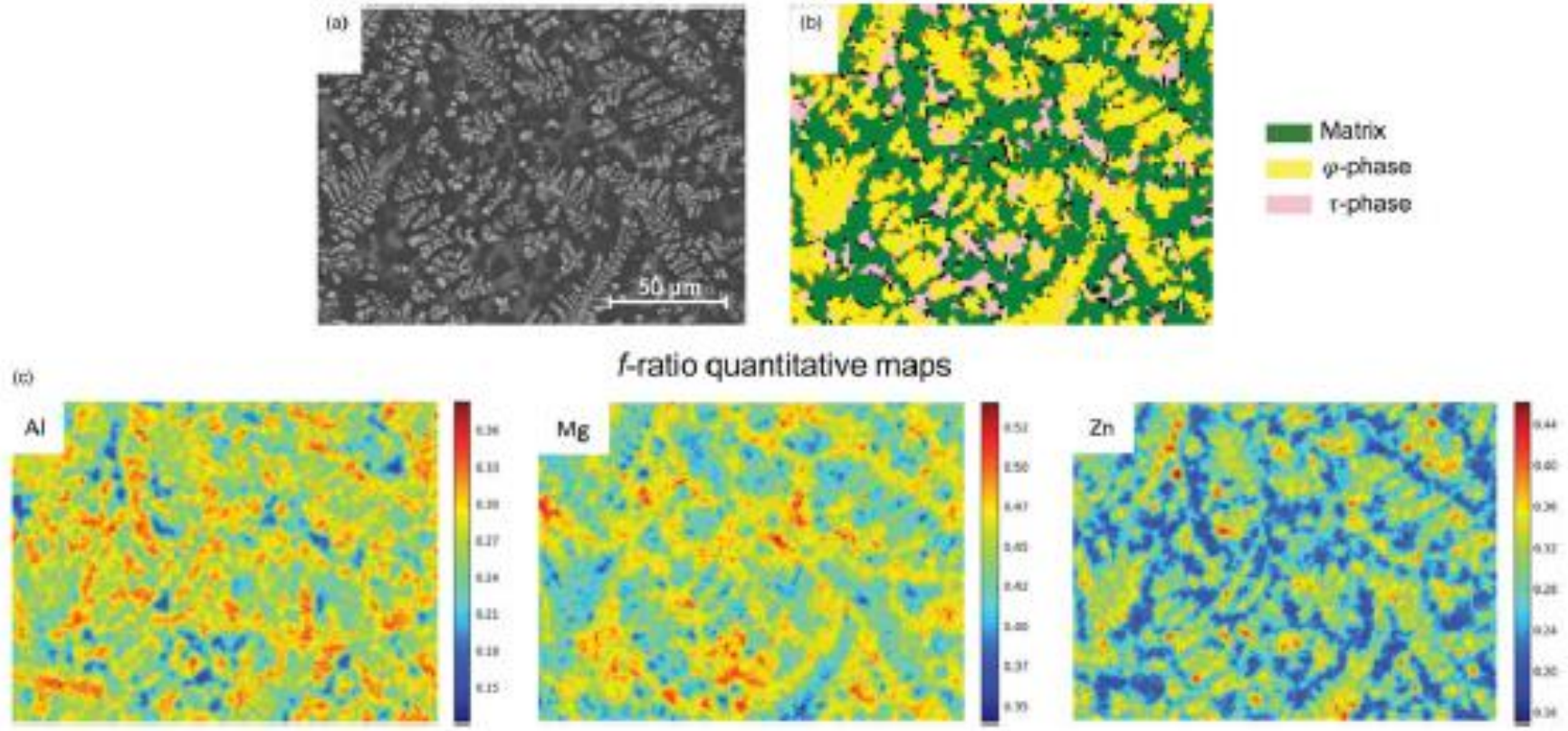

Available online at www.sciencedirect.com

ScienceDirect

Scripta Materialia 80 (2014) 41–44

Scripta MATERIALIA

www.elsevier.com/locate/scriptamat

Grain boundary diffusion of Al in Mg

Sazol Kumar Das, Nicolas Brodusch, Raynald Gauvin and In-Ho Jung*

Department of Mining and Materials Engineering, McGill University, 3610 University Street, Montreal, QC H3A 0C5, Canada

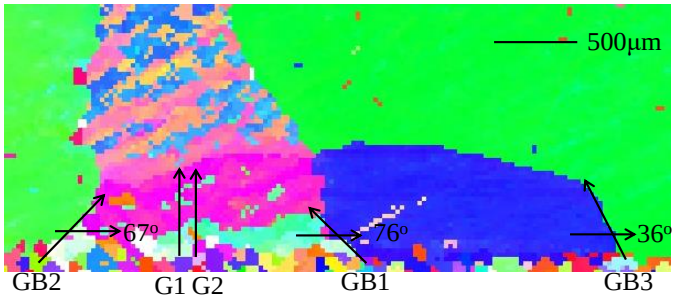

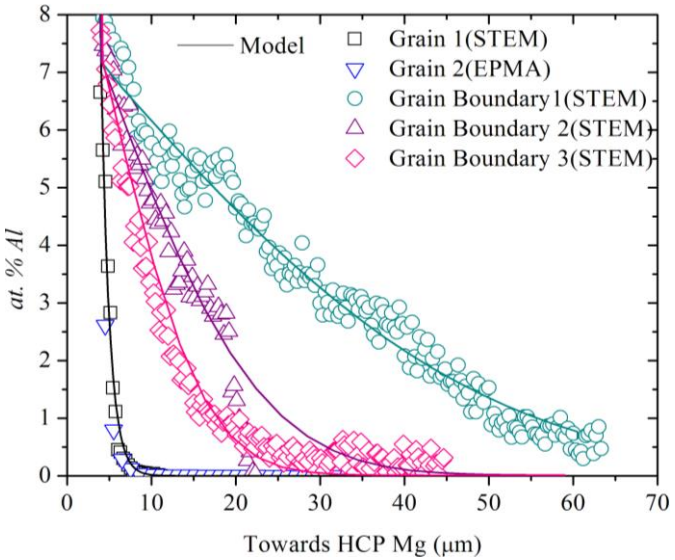

$$D = D_0 e^{-\frac{Q}{KT}}$$

$$lnD = ln\left(D_0 e^{-\frac{Q}{KT}}\right)$$

$$lnD = lnD_0 - \frac{Q}{KT}$$

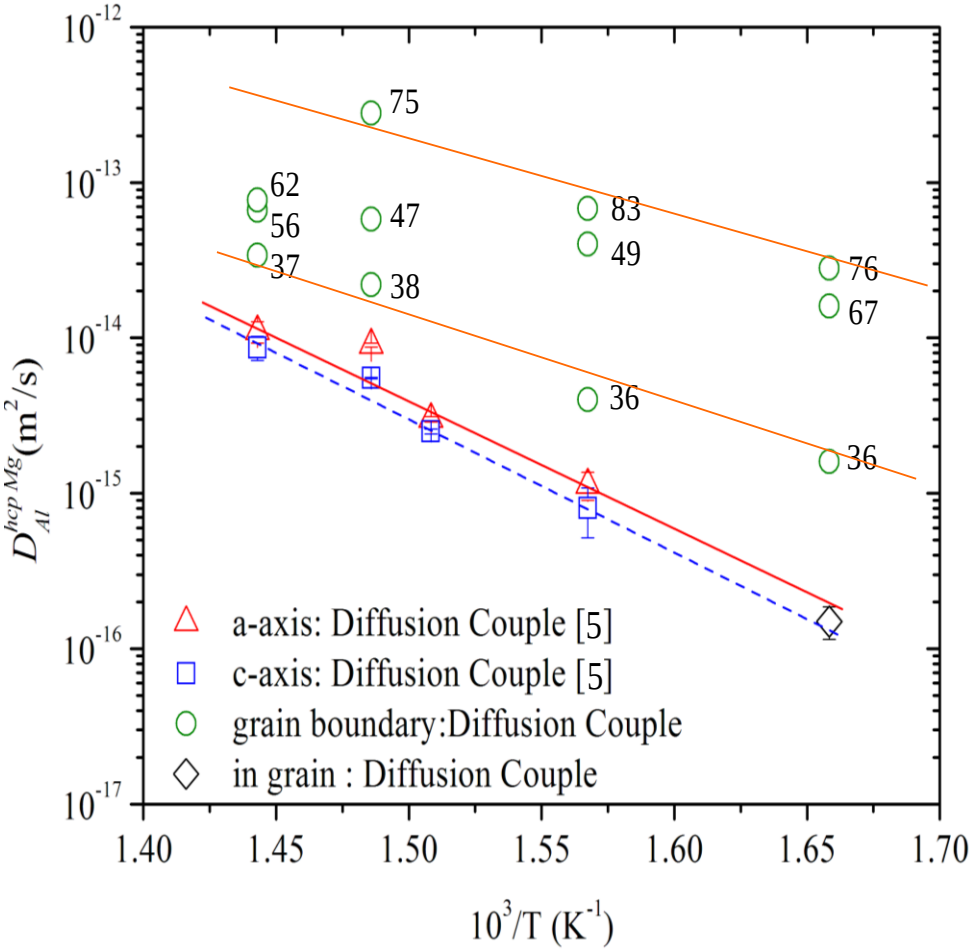

SU-9000EA STEM

Si, Plans (022), 30 keV

BF

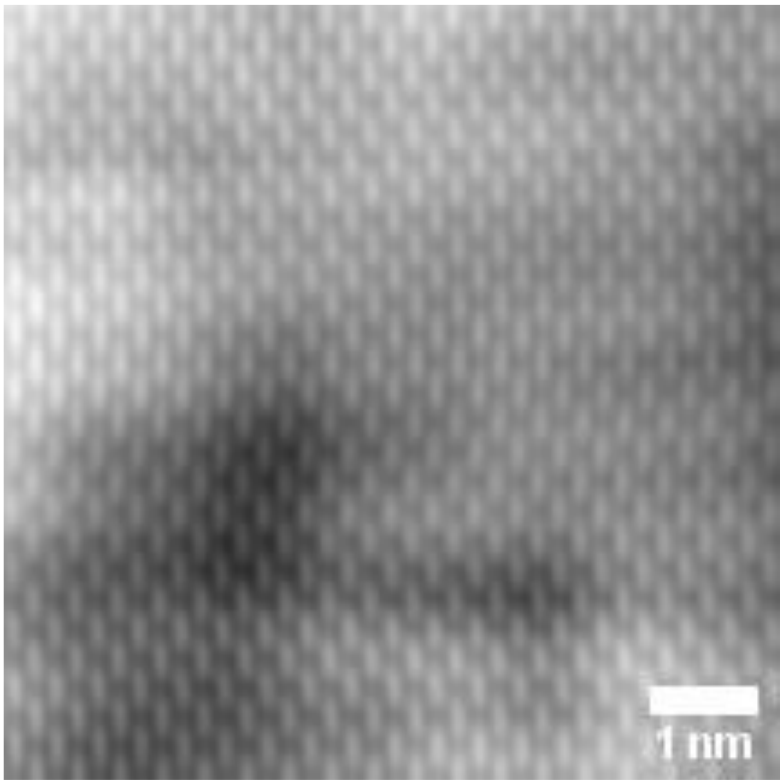

HAADF

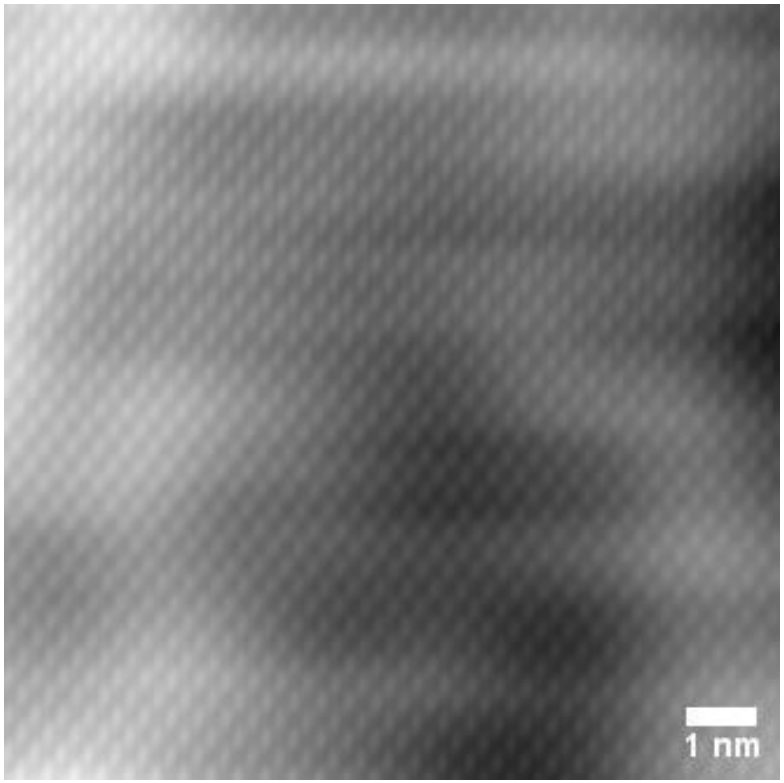

Espacement du réseau de 0,19 nm.

EDS X-Max Extreme d'Oxford
Angle solide de 0,78 Sr au SU-9000

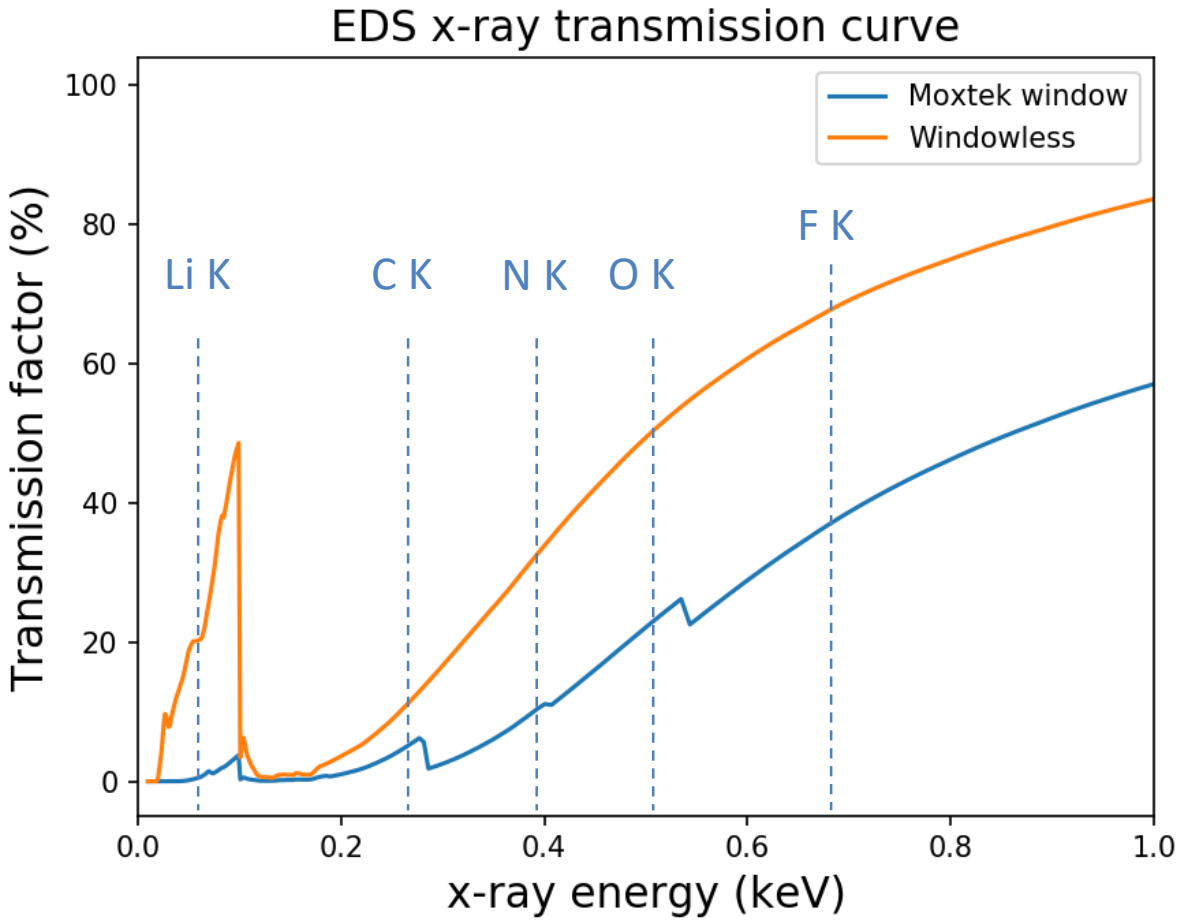

Imagerie de nanomatériaux par EDS à 30 kV (détecteur EDS sans fenêtre)

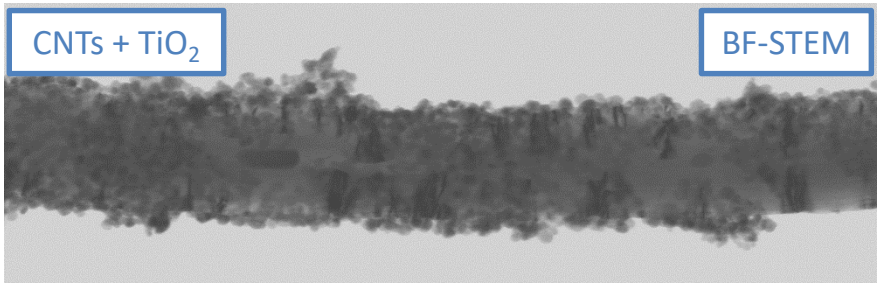

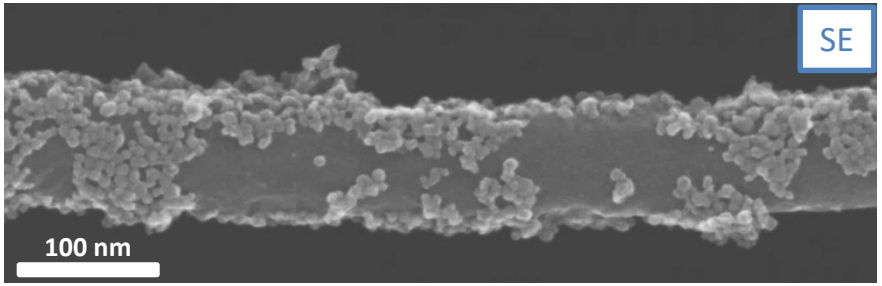

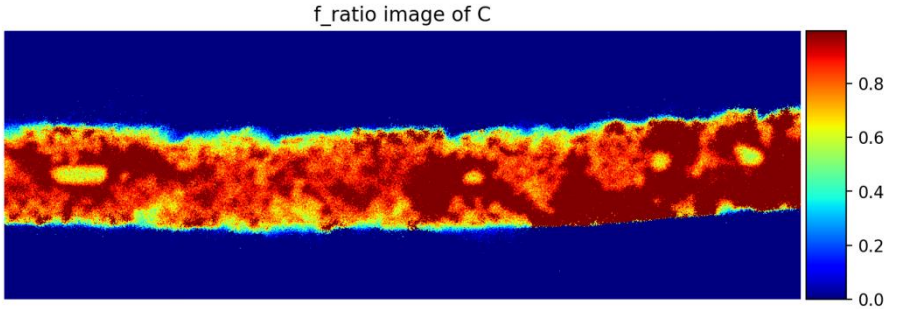

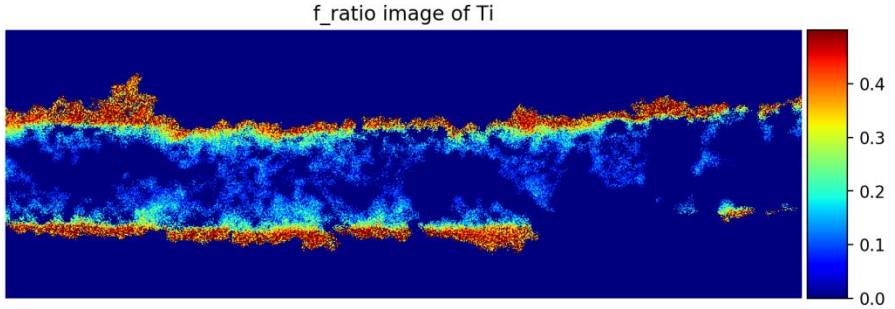

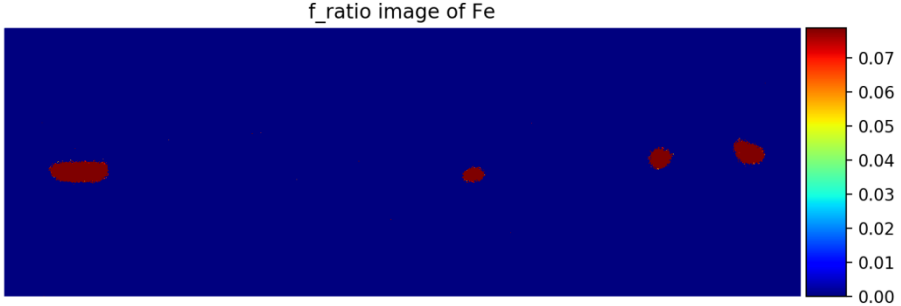

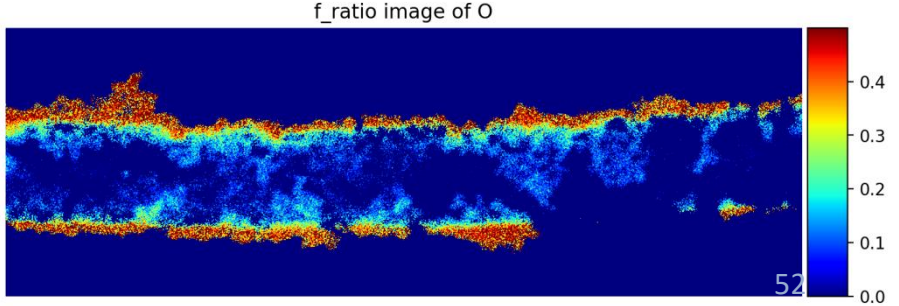

Analyses de surface par EDS à Très Bas Voltage

Anode LIB with SBR/CMC binder composite

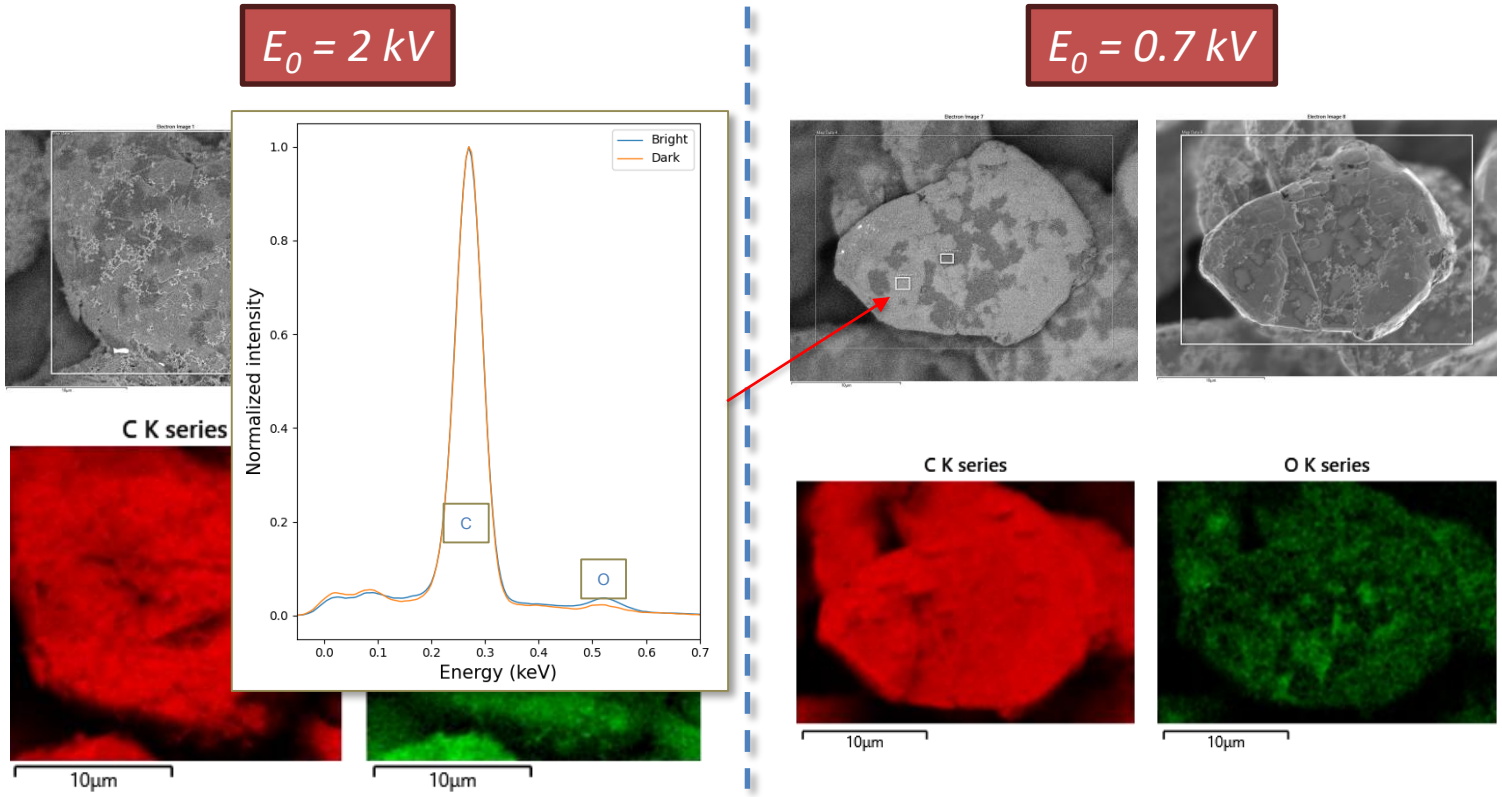

Electron Channelling

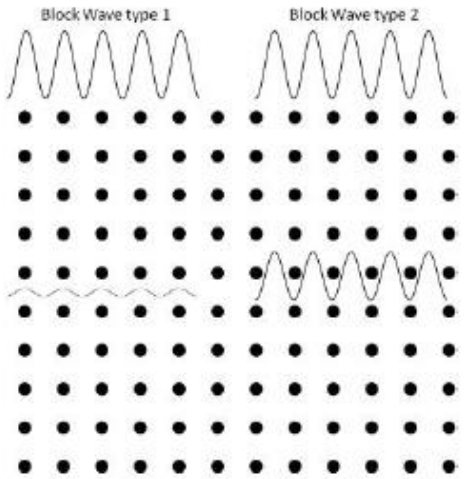

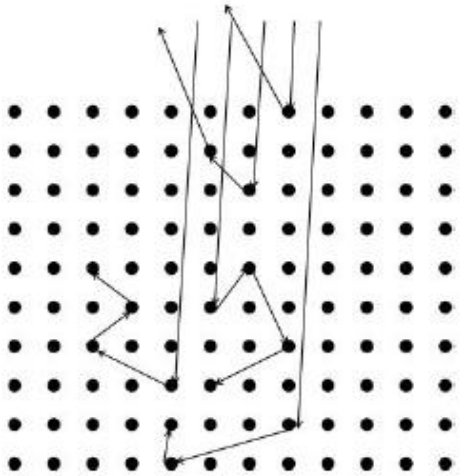

Low retrodiffusion yield

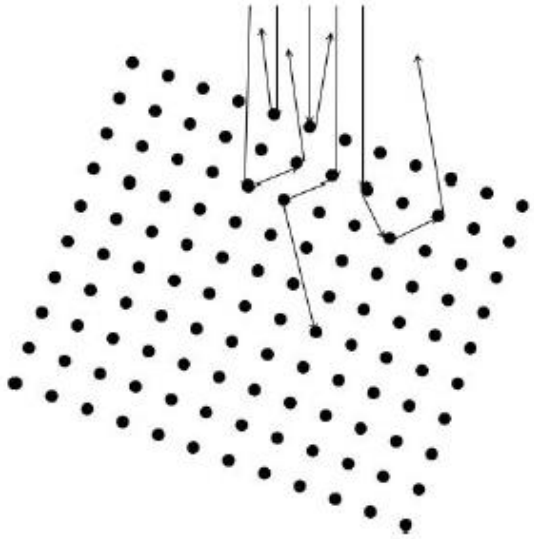

High retrodiffusion yield

Microsc. Microanal. 15, 83–92, 2009
doi:10.1017/S1431927609090242

Microscopy AND Microanalysis

Electron Channeling: A Problem for X-Ray Microanalysis in Materials Science

Frederick Meisenkothen,[1,*] Robert Wheeler,[1] Michael D. Uchic,[2] Robert D. Kerns,[1] and Frank J. Scheltens[1]

[1]*Air Force Research Laboratory, Materials Characterization Facility, operated by UES, Inc., Wright Patterson Air Force Base, OH 45433, USA*
[2]*Air Force Research Laboratory, Materials and Manufacturing Directorate, Metals Development Group, Wright Patterson Air Force Base, OH 45433, USA*

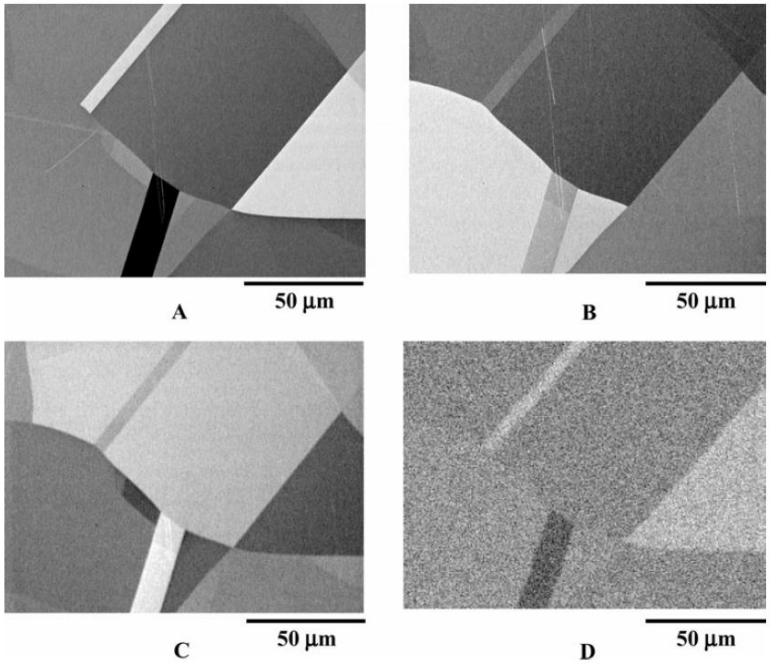

Figure 3. TaC polished by conventional metallographic stepped grinding/polishing schedule. Overvoltage is 1.06 (10.5 keV). **A:** Backscatter electron image at 0° tilt. **B:** Backscatter image at 5° tilt. The significant contrast changes that result from small specimen inclination changes is one way to verify that the contrast results from electron channeling effects. **C:** Backscatter image at 20° tilt. **D:** Ta$L\alpha$ WDS X-ray image, corresponding to image **A**. The average number of X-ray counts per pixel for the darkest contrast is 385, while the lightest contrast regions yielded an average of 450 counts (17% greater X-ray yield over the darkest grain).

Journal of Microscopy

Journal of Microscopy, Vol. 267, Issue 3 2017, pp. 288–298
doi: 10.1111/jmi.12565
Received 8 December 2016; accepted 21 March 2017

The qualitative f-ratio method applied to electron channelling-induced x-ray imaging with an annular silicon drift detector in a scanning electron microscope in the transmission mode

NICOLAS BRODUSCH & RAYNALD GAUVIN
Department of Mining and Materials Engineering, McGill University, Montréal, Québec, Canada

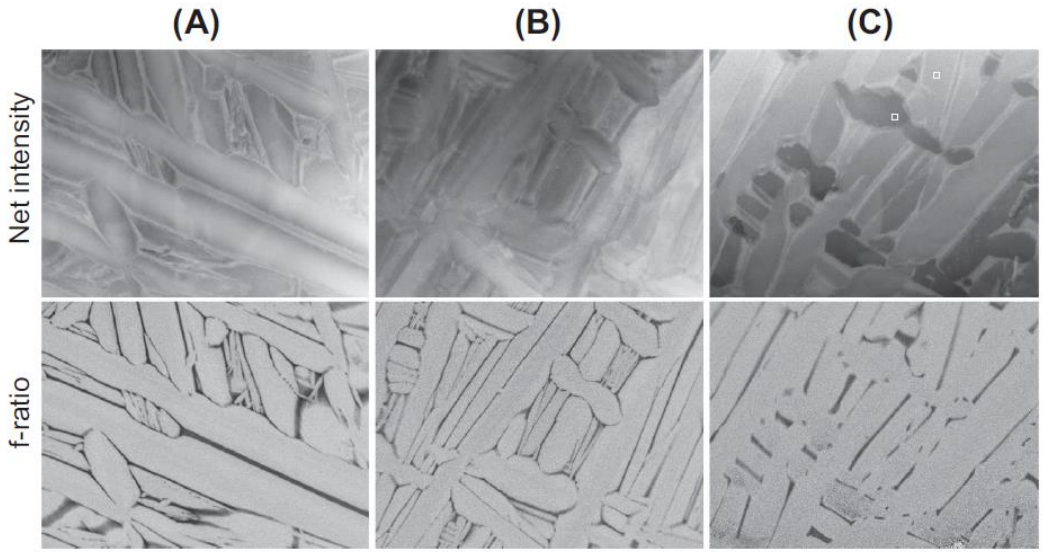

Fig. 1. Low magnification net intensity x-ray and corresponding f-ratio images of a Ti-6Al-4V thin specimen. (A)–(C) Net intensity x-ray images for Ti Kα (top) and corresponding f-ratio images (bottom). For the sake of clarity, only the Ti Kα images are shown. The effectiveness of the f-ratio method in cancelling the effects of specimen thickness (B) as well as defect density (A), (B) and channelling (C) is clearly demonstrated. The white squares in (C) mark the areas used to calculate the contrast between high and low channelling conditions.

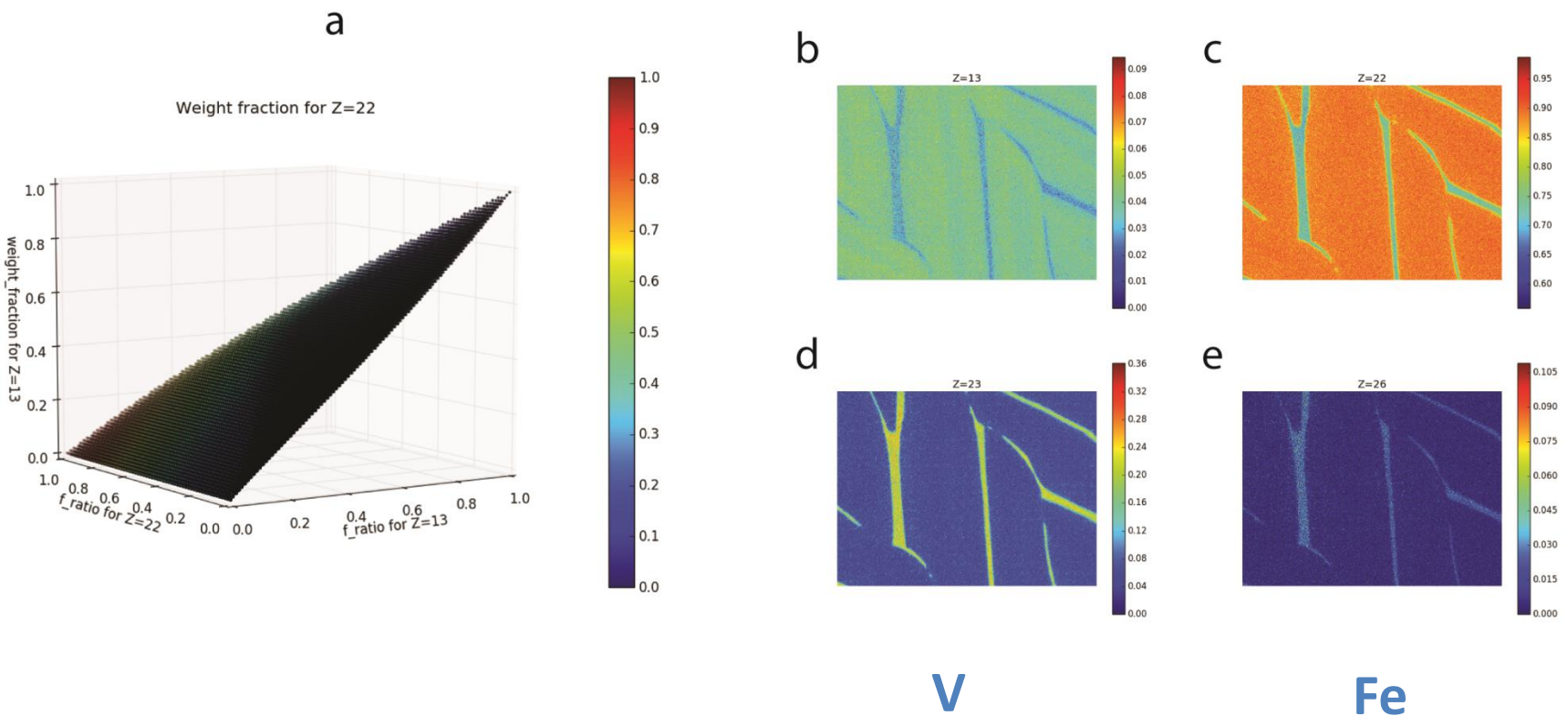
a
Weight fraction for Z=22
weight_fraction for Z=13
f_ratio for Z=22
f_ratio for Z=13
b
Z=13
c
Z=22
d
Z=23
e
Z=26
Al
Ti
V
Fe

Identification de Phases par Corrélation des Spectres EDS

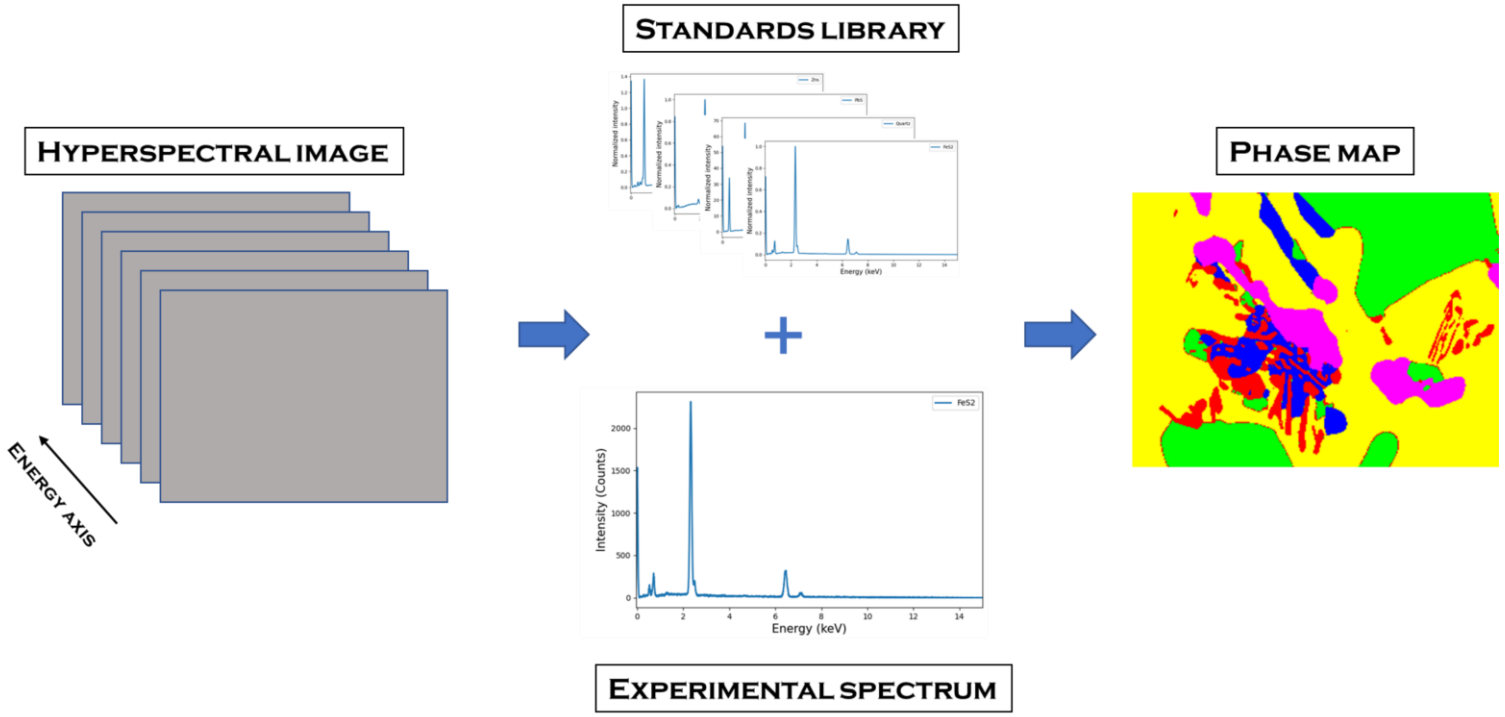

Ultramicroscopy 238 (2022) 113534

Contents lists available at ScienceDirect

Ultramicroscopy

journal homepage: www.elsevier.com/locate/ultramic

Phase differentiation based on x-ray energy spectrum correlation with an energy dispersive spectrometer (EDS)

Nicolas Brodusch *, Raynald Gauvin

McGill Electron Microscopy Research Group, Department of Mining and Materials Engineering, McGill University, Wong Building, 3610 University Street, Montréal, Québec H3A 0C5, Canada

Standards

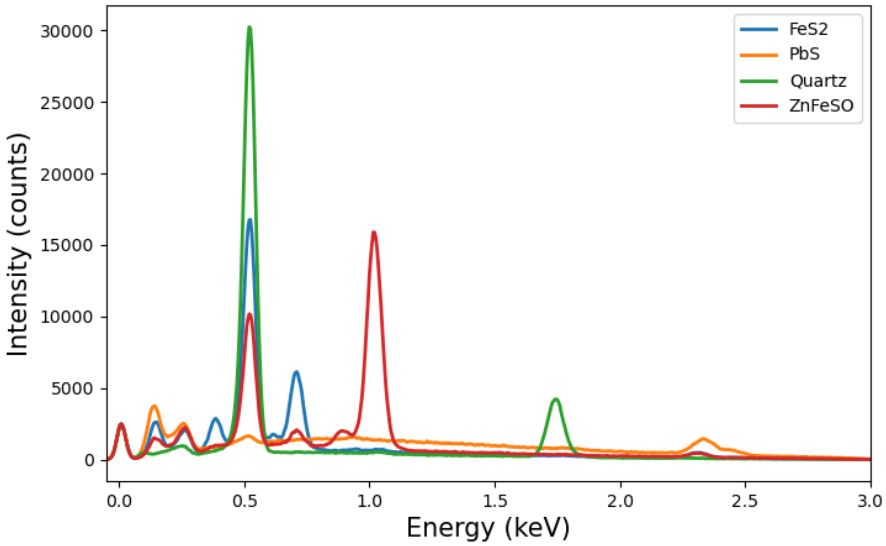

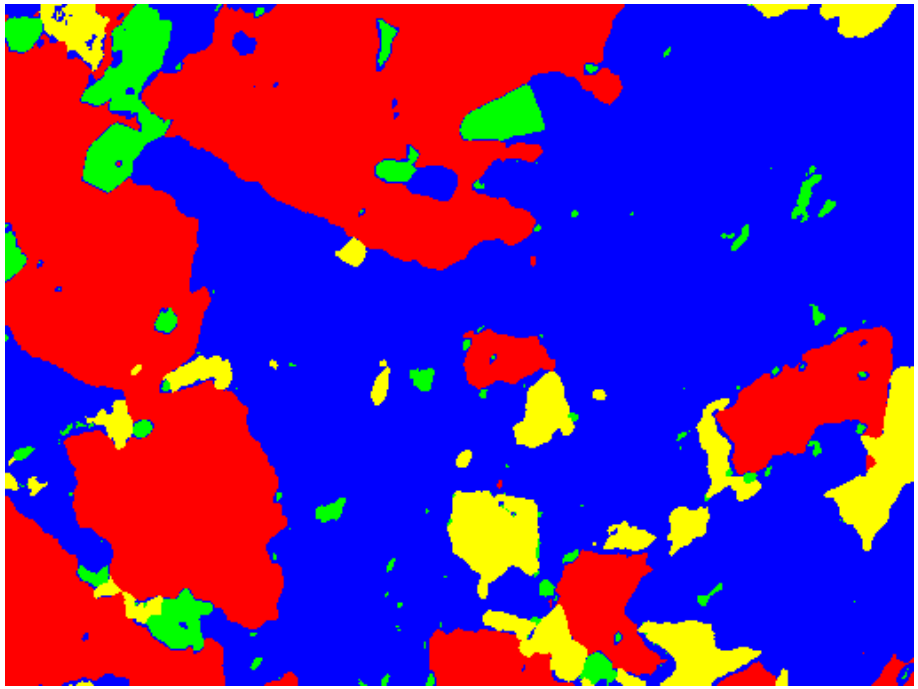

Cartes des Phases haute Résolution

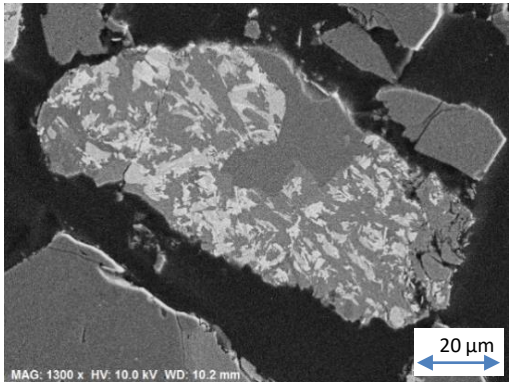

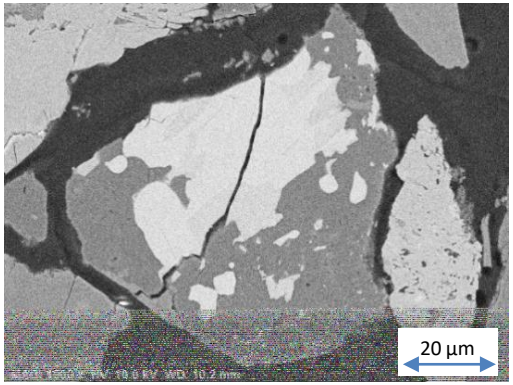

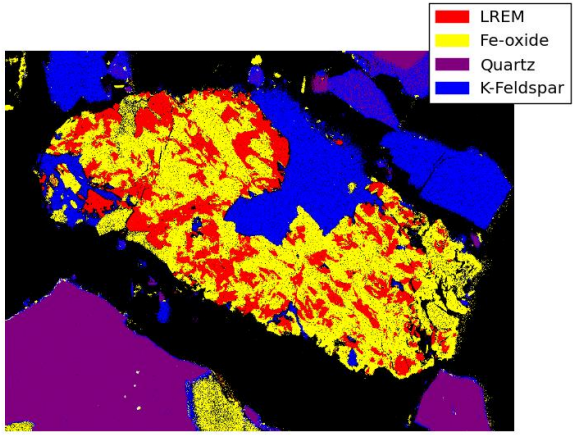

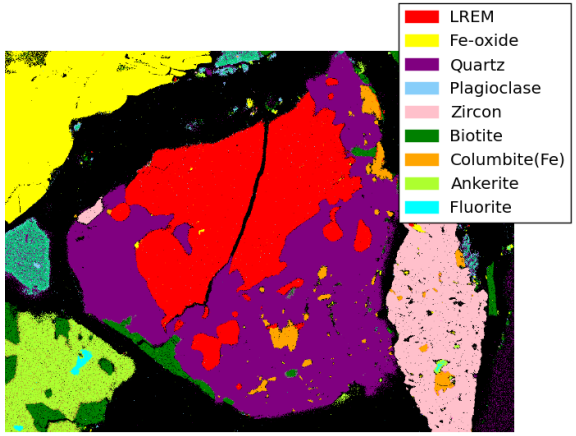

- Annular detector
- 10 kV, 20 min
- Magnification: 1500x

Cast Al-Mg-Zn alloy, 5 keV

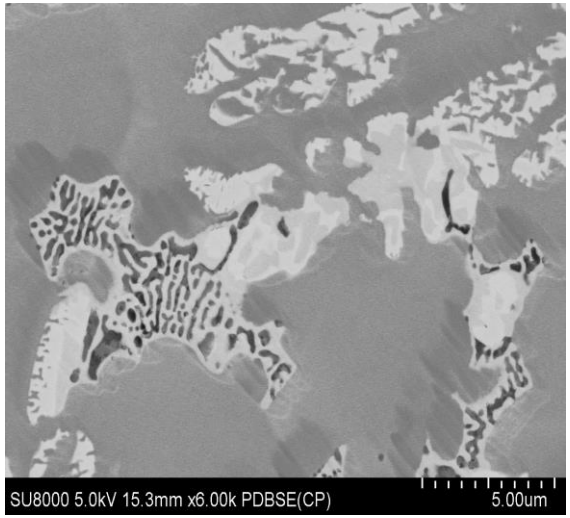

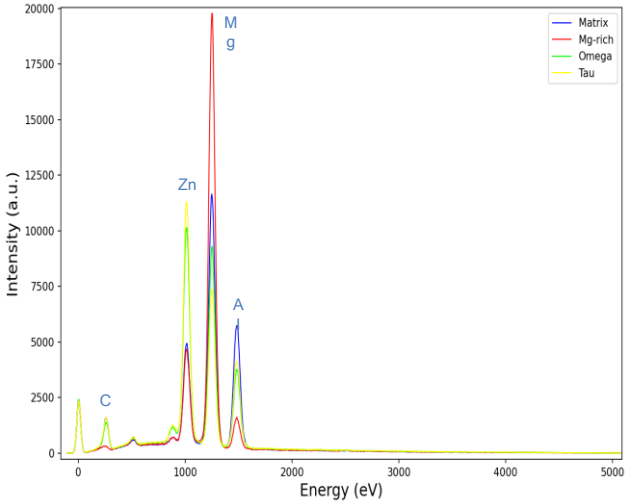

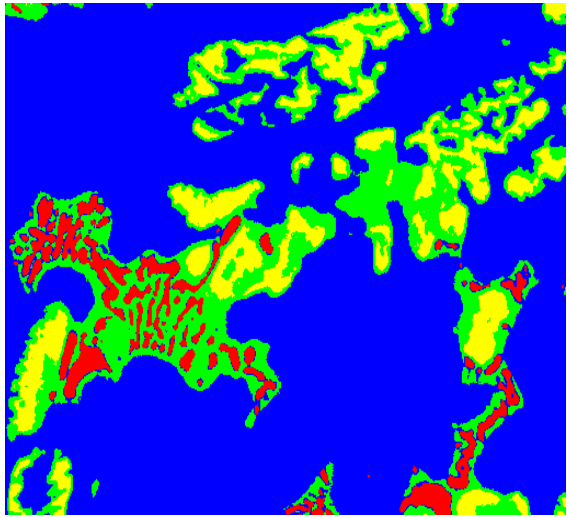

Energy & Environmental Science

ROYAL SOCIETY OF CHEMISTRY

PAPER

View Article Online
View Journal

Check for updates

Cite this: DOI: 10.1039/d4ee00551a

Nearly all-active-material cathodes free of nickel and cobalt for Li-ion batteries†

Eunryeol Lee, ‡[a] Dae-Hyung Lee,‡[ab] Stéphanie Bessette,[c] Sang-Wook Park,[ab] Nicolas Brodusch,[c] Gregory Lazaris,[c] Hojoon Kim,[ab] Rahul Malik,[d] Raynald Gauvin,[c] Dong-Hwa Seo *[ab] and Jinhyuk Lee *[c]

1.2 keV

a LMOF [90:5(MWCNT):5] (before cycling)

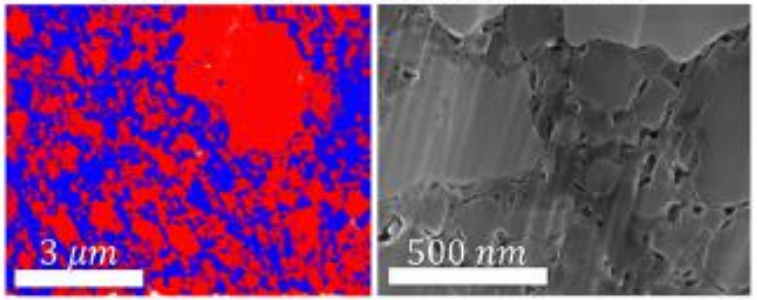

b LMOF [90:5(MWCNT):5] (after 5 cycles)

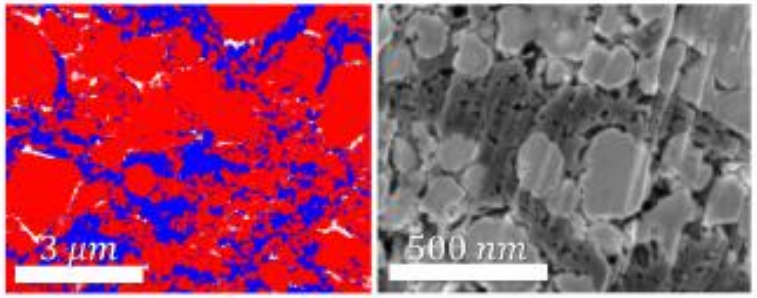

$Li_{1.68}Mn_{1.6}O_{3.7}F_{0.3}$

g

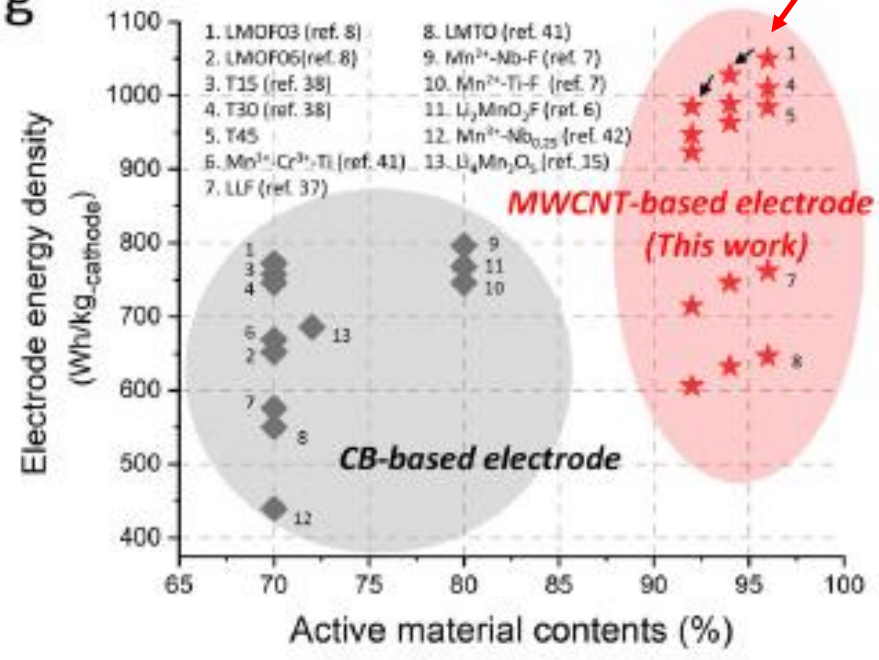

Pulvérisation Thermique d’un Super-Alliage de Ni

Lift-Out Massif par FIB-SEM (NX5000 FIB, SU9000EA – 2.5 keV)

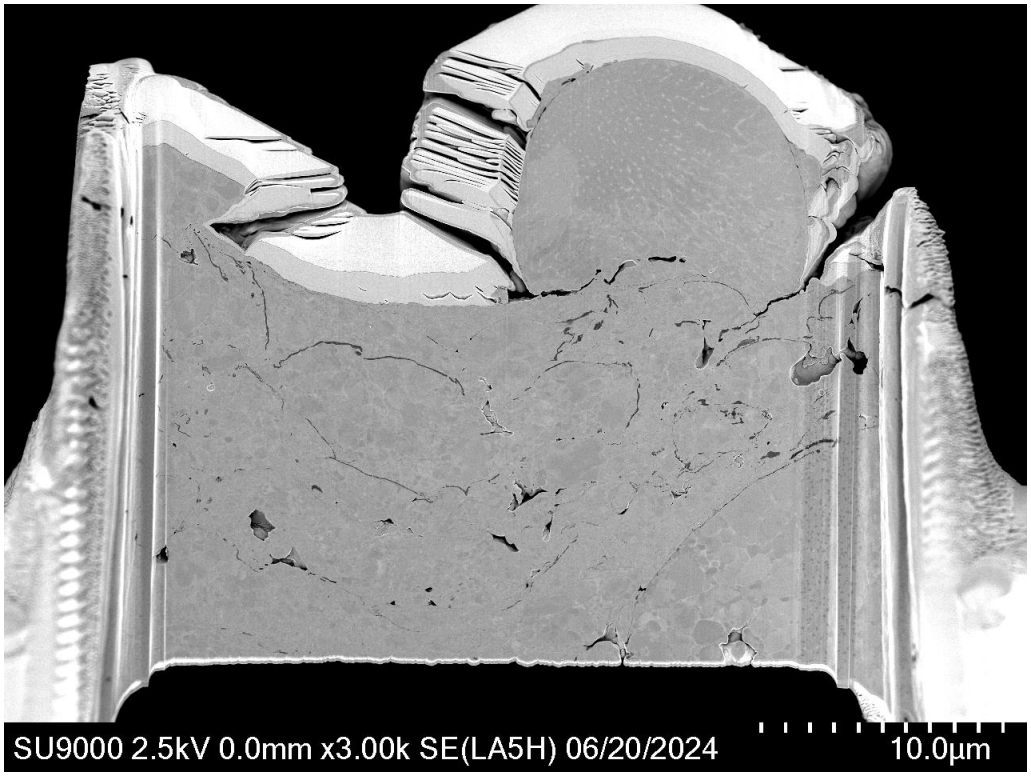

NX5000 FIB, SU9000EA – 2.5 keV

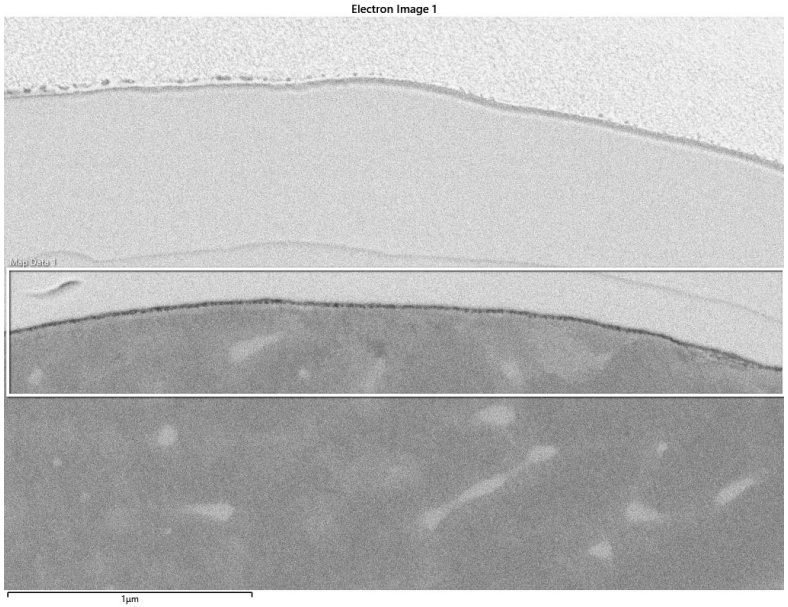

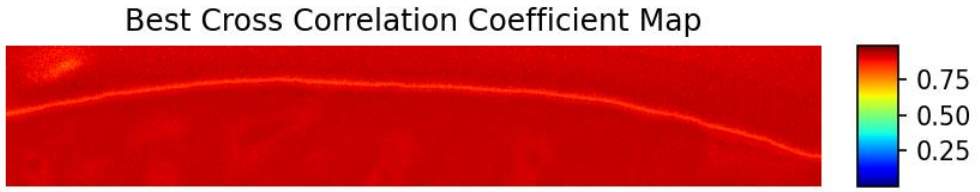

Raw

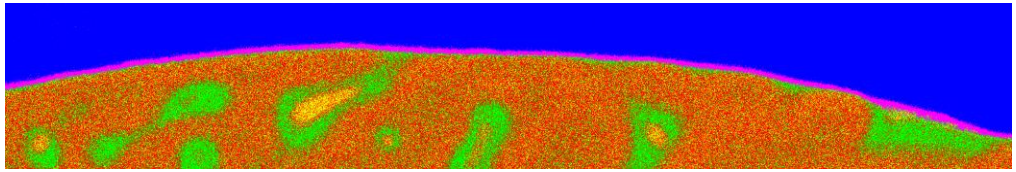

Smoothed

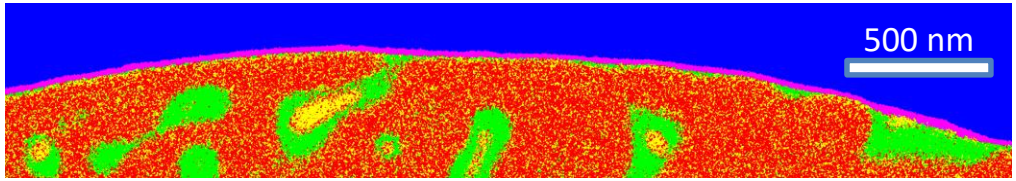

Phase Al-rich
Phase Ni-rich
Phase oxide
Phase Cr-rich
FIB Ga-C

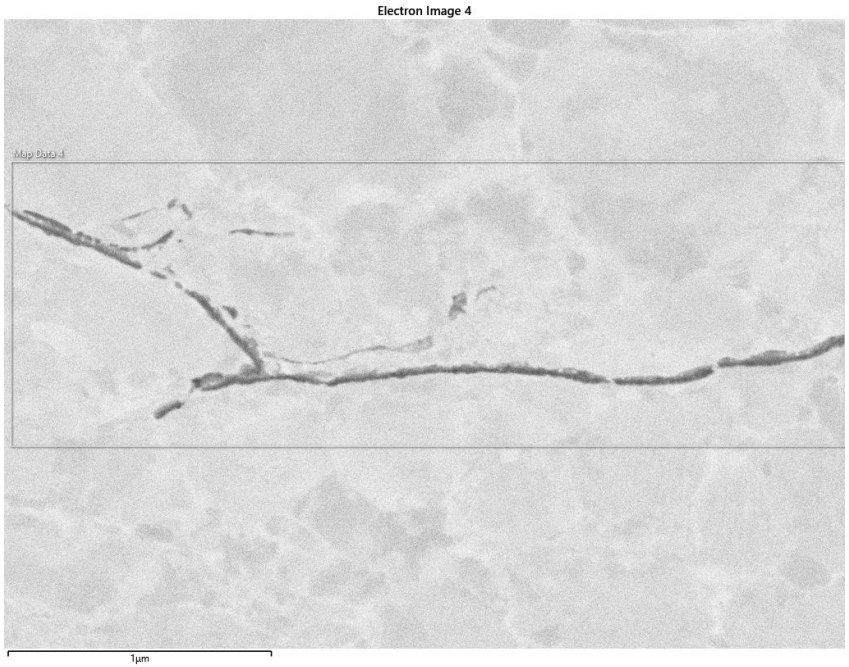

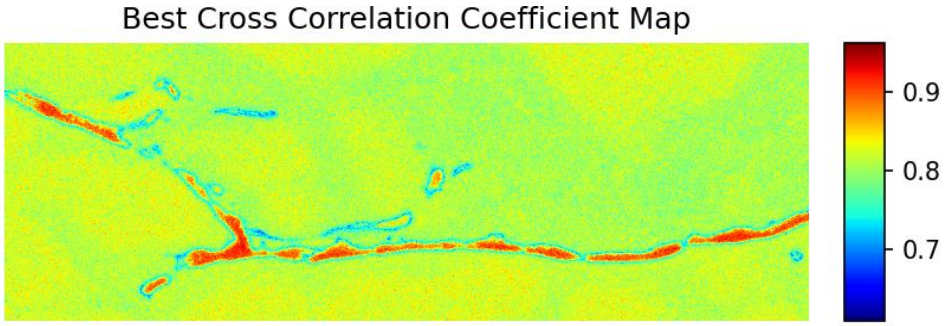

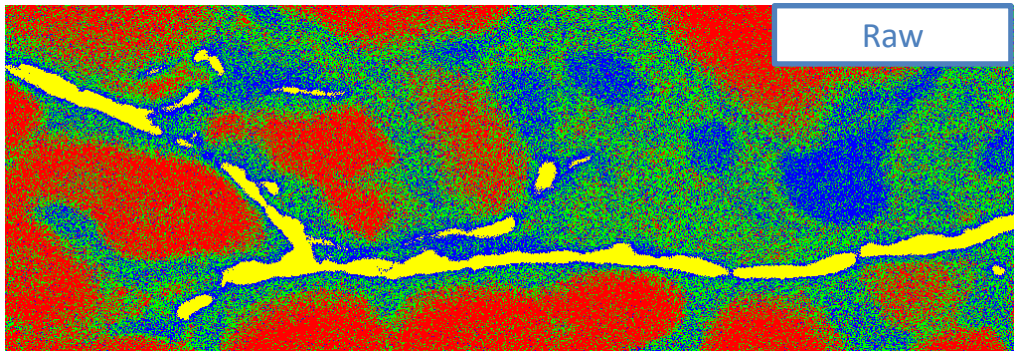

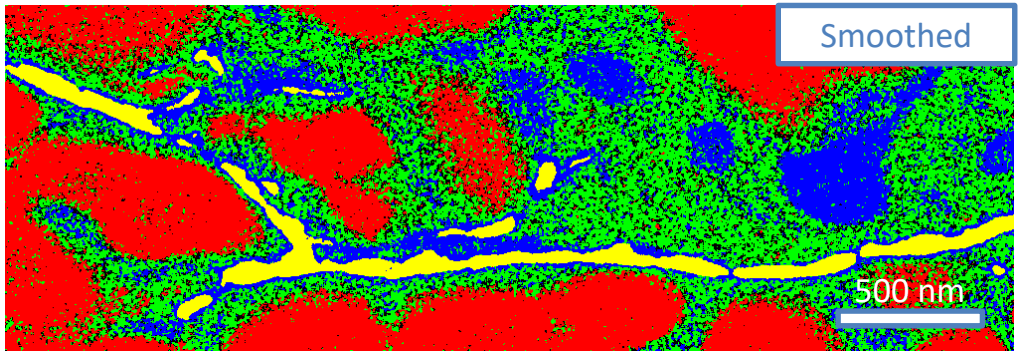

Phase Ni-rich

Phase oxide

Phase Cr-rich

Phase Ni-Cr rich


memrg.com